

CURRENT PROBLEMS IN MEDIUM RANGE FORECASTING AT ECMWF

DATA ASSIMILATION SCHEME

G.J. Cats

ECMWF

Abstract

A number of examples show that the analysis, made with the ECMWF data assimilation scheme, and/or the subsequent forecast with the ECMWF forecast model are sensitive to many parameters in the assimilation scheme. Because several of those parameters are not very well known (both qualitatively and quantitatively) this sensitivity poses a severe problem to medium range weather forecasting at ECMWF. The sensitivity is particularly related to insufficiency of accurate observational data.

1. INTRODUCTION

A medium range weather forecast is made by running an atmospheric model starting from some initial state of the atmosphere. The initial state is partly described by observations, but the density and accuracy of the observations are not sufficient to define the initial state uniquely. Therefore an analysis is made, which at ECMWF is an update of the atmospheric fields as forecast by the ECMWF model, using the available data. In the analysis scheme many parameters occur, and most of them are not known accurately. Their values have been chosen only to produce reasonable analyses over a large ensemble of cases. A huge problem in medium range weather forecasting, however, is that the forecast is often very sensitive to the precise choice of those parameters.

In this paper a number of examples of such sensitivity in the ECMWF model will be given. The examples relate to two types of sensitivity. The first type shows that the initial state is often sensitive to the parameters used to construct it. It is no surprise that in those cases the forecast is

sensitive as well. Of the second type are the examples where the initial state is hardly affected by the choice of the parameters (at least, in its height, wind, temperature etc. fields) but where the forecast is yet very sensitive to the parameters.

The first type of sensitivity is usually due to the data checking algorithm, which determines whether a datum is correct (in which case it is accepted) or incorrect (in which case it is rejected). A slight change of a parameter in the analysis scheme may cause the rejection of a datum that was previously accepted or vice versa. The examples relating to this mechanism are collected in the next section. Sensitivities of the first type are sometimes due to other mechanisms, e.g., a small change in static stability in an analysis may trigger convection during a six hour forecast. The forecast fields are used in the next analysis, and if there are no relevant observations in that analysis the analysed fields may alter considerably. Some examples of this kind of sensitivity are shown in the third section.

The second type of sensitivity gives an impression of the accuracy of the analysed fields which is required by the ECMWF forecast model. Examples are described in the fourth section.

For most of the examples a reasonable understanding of the ECMWF data assimilation scheme is useful. Some explanations will be given with each example. A few general remarks on the scheme follow.

The ECMWF data assimilation scheme consist of a repeating sequence of analysis, initialization and six hour forecasts, together called a data assimilation cycle. The forecast, made with the ECMWF forecast model, produces the "first-guess" fields for the next analysis. The analysis mixes information from the first guess field with that from the observations. The

observations that are used are from as many sources as practicable. Height, wind, thickness/temperature and humidity observations within a six hour time window centered around the analysis time are considered. The height and wind analysis is three-dimensional, multivariate and based on the optimum interpolation technique (Lorenz 1981). The humidity is analysed with a correction method. Surface parameters (e.g. soil moisture and temperature at the soil surface and at a depth of 1 m) are not analysed yet; instead they are replaced by assumed climatological values (apart from soil surface temperature which is taken from the first-guess). The height, wind and humidity are analysed on 15 standard pressure levels, and a vertical interpolation is required to get the analyses on the 15 model σ -levels. The analysed height fields are transformed to temperature fields as required by the model with the hydrostatic equation. In the present operational implementation these fields on σ levels are not changed by the analysis if there are no observations. The initialization scheme has been described by Williamson and Temperton (1981). A summary of the main features of the assimilation scheme is given in Appendix A.

The sensitivity of the forecast to the initial state, and of the initial state to parameters in the data assimilation scheme, renders it impossible to judge the quality of a change in the assimilation scheme from inspection of the meteorological charts of the analysis or from the quality of a small number of test forecasts. Instead, one would require a large sample to assess the average effect of a change. This, however, would greatly exceed available computer and manpower resources. At ECMWF, the quality of the operational forecasts is monitored with objective measures. During the second year of operational forecasting (1980/1981) that quality has improved consistently over that during the first year. Although this improvement might partly be due to the difference in synoptic situations and in data availability, it is felt that it is also at least partly attributable to the large number of changes that have been introduced in the analysis scheme in

the beginning of the second operational year. Only now, after a long period of operational quality assessments, we feel justified to say that the analysis scheme changes constituted improvements.

2. SENSITIVITY THROUGH DATA CHECKING

2.1 Description of data checking algorithm

In the analysis scheme every observed datum undergoes several checks before it is used for the final analysis. For the mass and wind analysis the final check, that is preceded by checks on internal consistency, agreement with nearby data and agreement with a first guess value, is carried out as follows.

The data are grouped into "boxes" of about 660 x 660 km². Each datum within a box is compared to a preliminary analysis which avoids the use of any datum already rejected and which also avoids the use of the datum that is being checked. The deviation of the observed value from the preliminary analysis value is expressed in terms of the dimensionless ratio q :

$$q = \frac{(\sigma - a_p)^2}{e_{ap}^2 + e_\sigma^2} \quad (1)$$

where σ is the observed value, a_p the preliminary analysis, e_{ap} an estimate of the error in that analysis, and e_σ an estimate of the observation error.

If for any datum within the box q exceeds q_{lim} (at present 16) the datum with the highest q -value is rejected. This entire process is repeated until for each datum $q \leq q_{lim}$. After this has been done for all boxes, the mass and wind fields are analysed using only accepted (non rejected) data.

Sensitivity to any parameter in the analysis scheme reveals itself through the rejection or acceptance of data with the ratio q very close to q_{lim} . If, for example, a small (order ϵ) change in a parameter, with an associated change in a_p of order ϵ , reduces q from $q_{lim} + \epsilon$ to q_{lim} , a datum, previously rejected, will become accepted. Since such a datum is on the border of being rejected, q is large ($q \approx q_{lim}$) and therefore it deviates much from the preliminary analysis. Its inclusion will therefore change the analysis considerably.

The change in the final analysis is estimated as $d = w (\sigma - a_p)$ where w is the weight of the "doubtful" datum, if accepted. Because $q \approx q_{lim}$, $|d|$ is approximately

$$|d| \approx |w| \sqrt{q_{lim} (e_{ap}^2 + e_{\sigma}^2)} \quad (2)$$

The weight w is large if e_{σ} is small, so that in data sparse areas (large e_{ap}) $|d|$ may become very large. In the next part of this section two examples will highlight this effect in data sparse areas, and one will indicate that in data dense areas there is no such sensitivity. For the first example the actual change that made the rejection scheme treat the data differently is described. The other two cases arose from analyses where many parameters had been changed mainly due to round-off effects, so that these cases indicate the importance of the least significant bits in the computations.

2.2 Examples

2.2.1 First example: choice between two data

The first example, shown in Fig. 1 is from a case where a SHIP and a TEMP report at almost the same position have contradictory data for the height of the 1000 mbar level: The TEMP, call sign EREBO, reported -17 m, but the SHIP, call sign EREBO (!), reported 992 mbar for mean sea level pressure (MSLP).

38 SYNOP/SHIP 14 TEMP 12 GMT 7 September 1980
 1000 mb First-Guess Geopotential Height

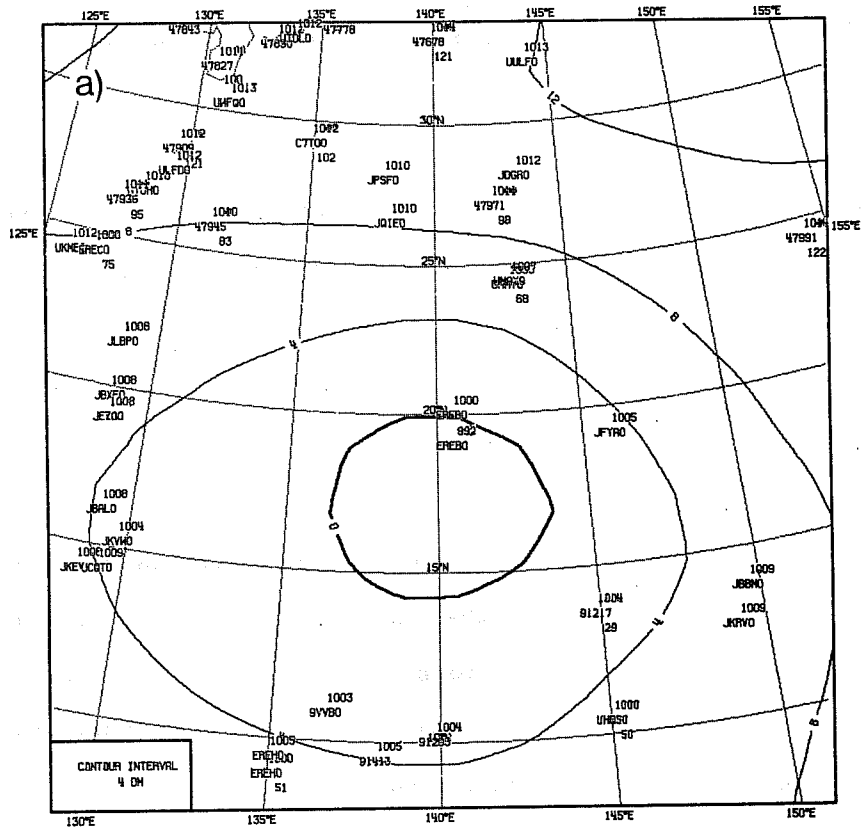
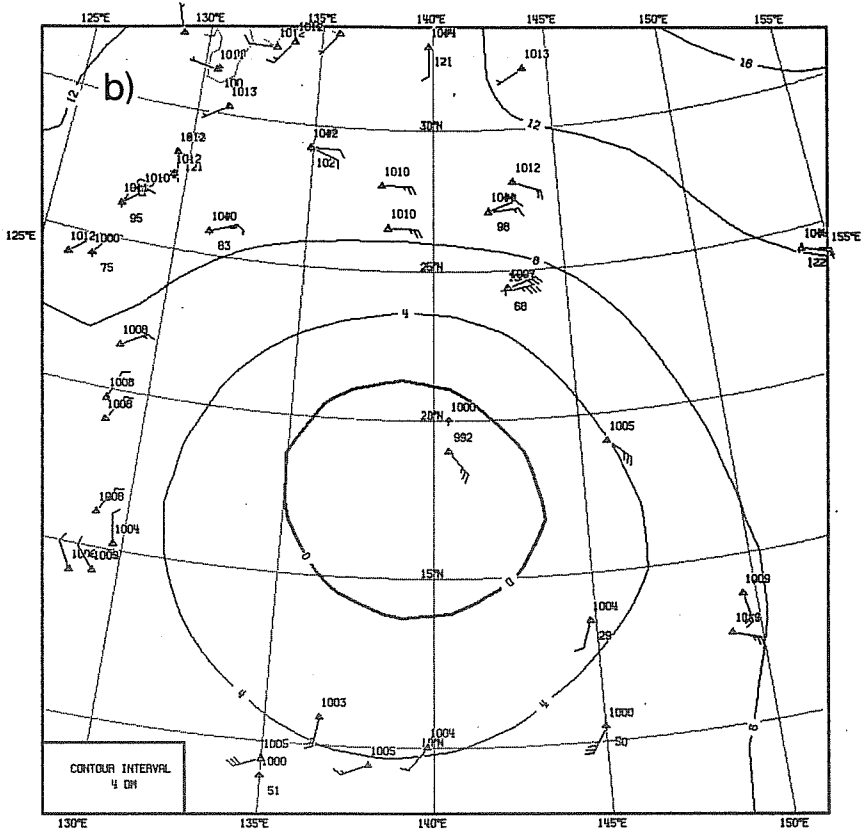


Fig. 1 First guess (a) and two analyses (b,c) for 12 GMT 7 September 1980. In analysis (b) the TEMP report EREBO of -17m for the 1000mb height has been accepted, in analysis (c) the SYNOP report EREBO of 992mb for the mean sea level pressure.

12 GMT 7 September 1980

1000 mb Analysed Geopotential Height



1000 mb Analysed Geopotential Height

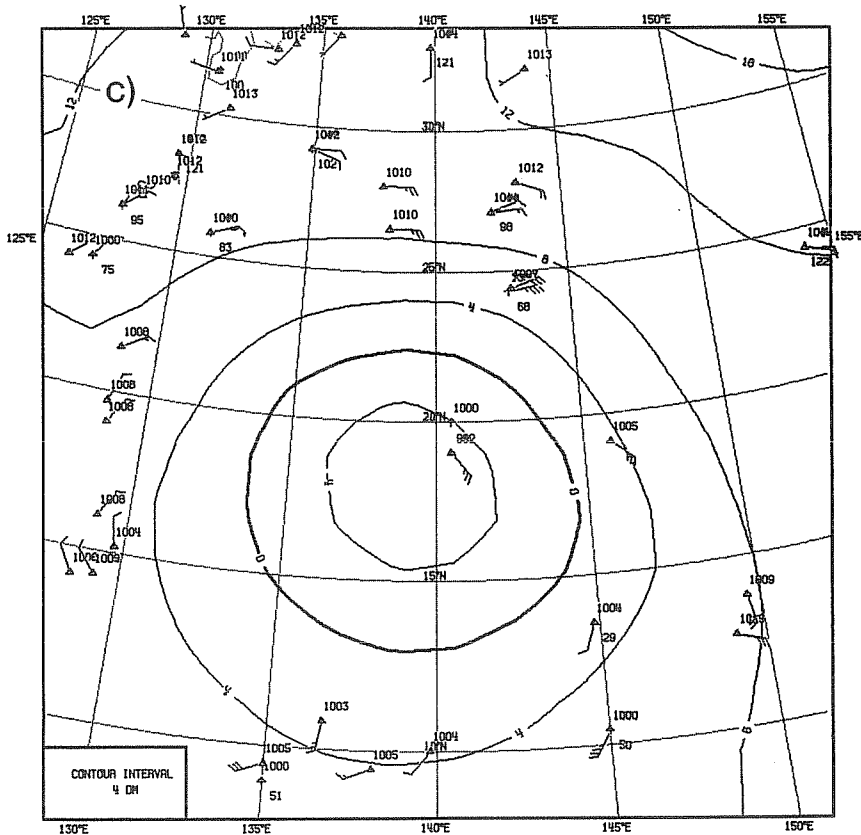


Fig. 1 (cont.)

In the analysis scheme, a correlation between the height observation errors within a single TEMP report is assumed. At present, not enough statistics exist on the root-mean-square height observation errors, let alone on the correlations between these errors. In an analysis using the assumed value of 55% for the correlation between 850 mbar and 1000 mbar height observation errors, the TEMP report is accepted, and the SHIP rejected (Fig. 1b). If that correlation is reduced by 20%, the roles of the TEMP and SHIP reports are swapped (Fig. 1c), resulting in an MSLP change of 4 1/2 mbar.

A case like this is neither exceptional in frequency of occurrence, nor in data distribution, as can be seen already from many other similar contradicting coinciding TEMP and SHIP's in Fig. 1. Experience at ECMWF shows that for whatever change is made in the analysis scheme there is often a point on the globe where the resulting final analysis changes disproportionately.

2.2.2 Second example: data dense area

The second example shows that in a data dense area one can hardly see the effect of the acceptance or rejection of a single datum. In the analysis shown in Fig. 2a, a SYNOP report (longitude 67.1°W, latitude 68.1°S) of MSLP of 978 mbar has been used, whereas it was rejected for the analysis of Fig. 2b. The two MSLP analyses are very similar. It should be borne in mind, however, that other quantities, such as static stability or advection, being first or second derivatives of the height field, may differ enough to yield substantially different 10-day forecasts.

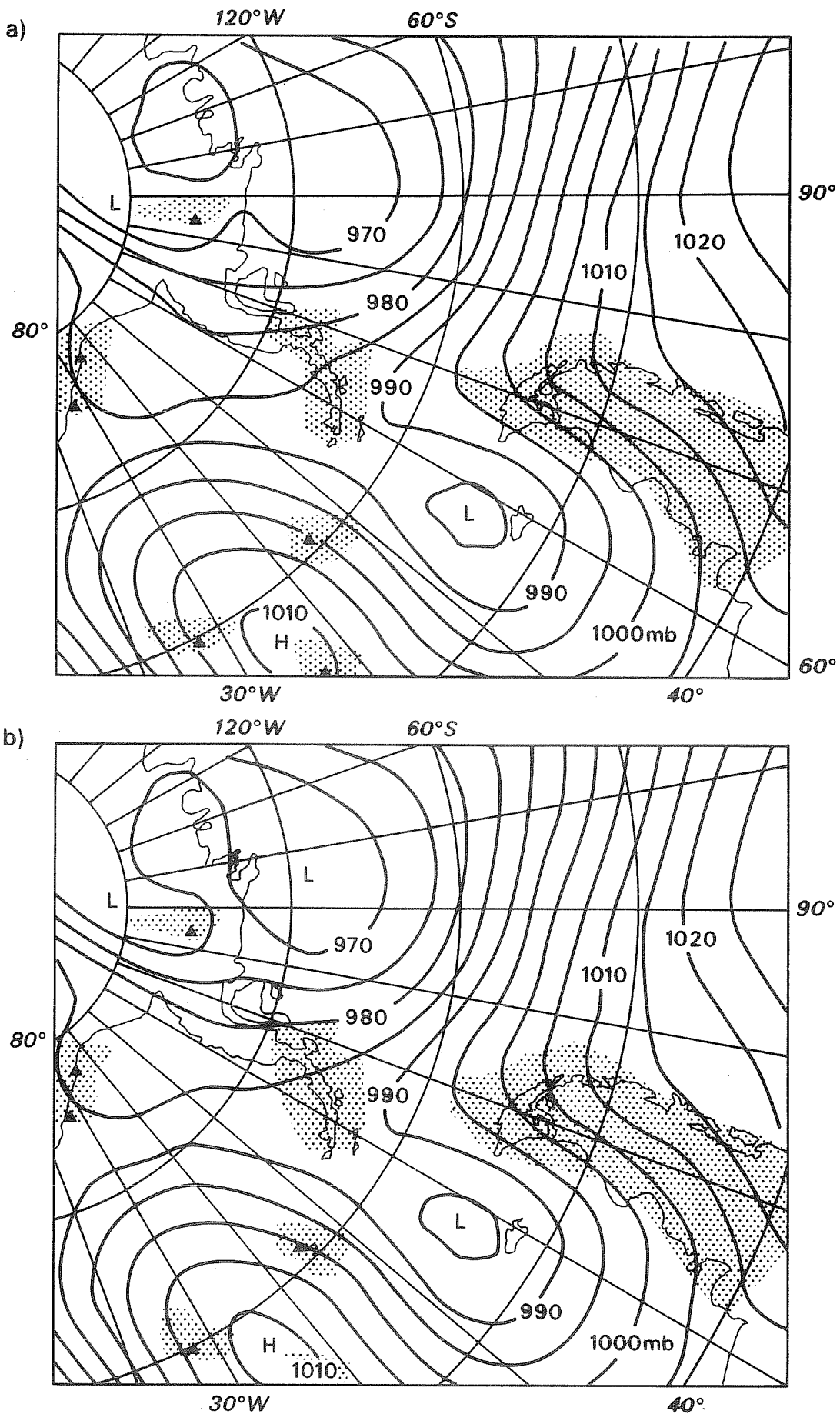


Fig. 2 Analysed mean sea level pressure near the Antarctic Peninsula for 1200 GMT 7 September 1980. In analysis (a) a SYNOP report of 978 mb mean sea level pressure on the peninsula has been accepted, which in analysis (b) has been rejected. Data dense areas have been shaded.

2.2.3 Third example: one isolated datum

The third example is again a situation on the southern hemisphere. The MSLP of SHIP GWAN has been rejected by the analysis of Fig. 3a. (This analysis is an operational ECMWF analysis). Because the area has few other data, accepting that datum (Fig. 3b) produces a markedly different analysis of the ridge along 100°W. From both analyses a forecast has been made. The two-day and four-day forecasts are shown in Fig. 4 and 5, respectively, together with the verifying analyses. The stronger ridge of the analysis of Fig. 3b can be followed through the forecast, to produce a strong high over South America. The verifying analyses show it as well, although they have been obtained with the ECMWF operational scheme, that is, after a sequence of assimilation cycles which started from the operational analysis shown in Fig. 3a.

This case is particularly suited to illustrate the effect of one datum on the forecast because the datum is in a data sparse region (so the analysis changes considerably) but the effects in the forecast occur over a data dense area (so that the verifying analyses are reliable).

The two forecasts in this case were made from analyses obtained with slightly different data assimilation schemes. Therefore the analyses differed not only in the treatment of this one datum. In Section 4 an experiment will be described in which the forecasts were run from analyses that differed in that respect only.

3. SENSITIVITY TO ANALYSIS ASPECTS OTHER THAN DATA CHECKING

3.1 Introduction

In this section several steps in the Data Assimilation Scheme will be looked at, in connection with sensitivity of the 10-day forecast to parameters in those steps. The first step in the ECMWF data assimilation scheme is the construction of a first guess field from a six hour forecast from the previous analysis. Because the model keeps temperature on sigma levels (see

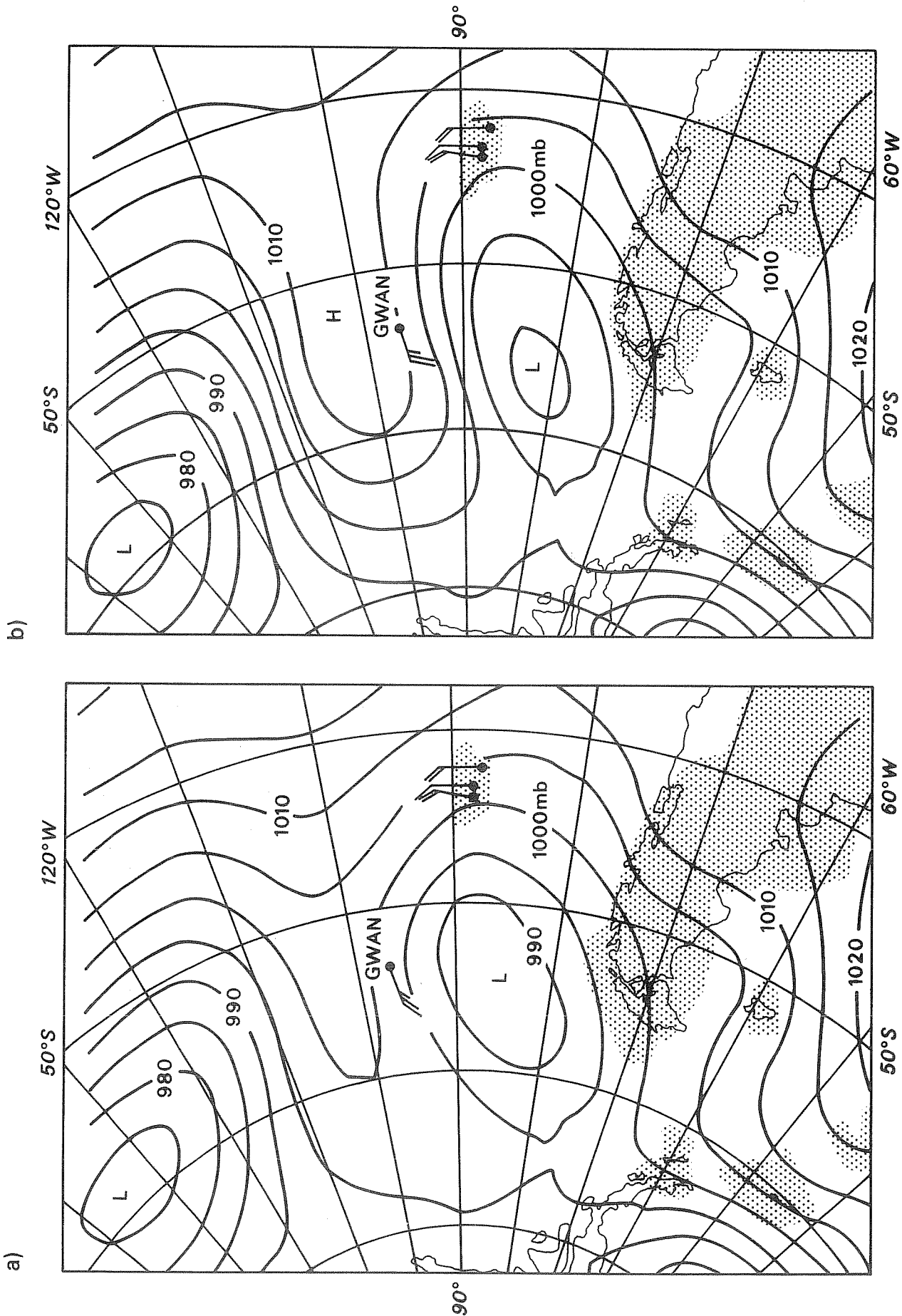
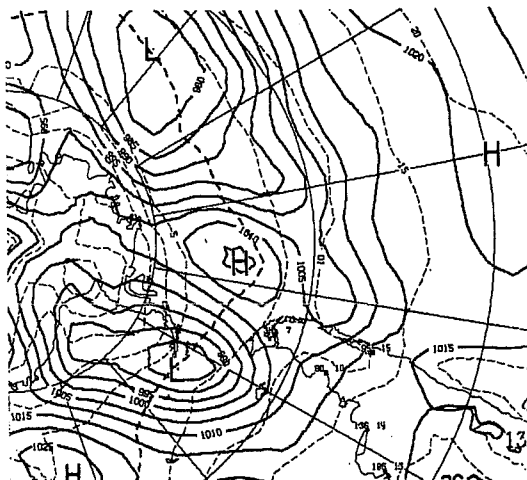


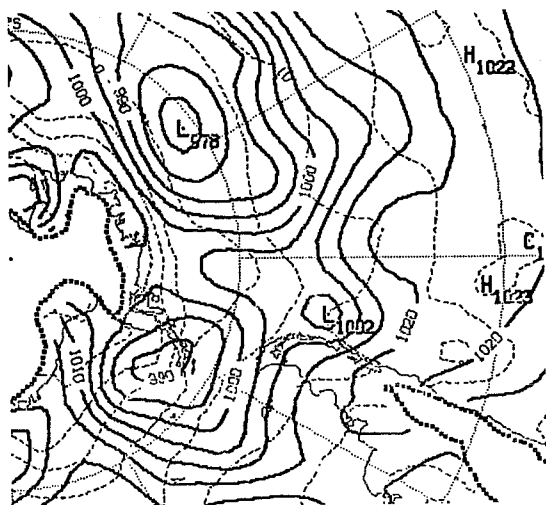
Fig. 3 Analysed mean sea level pressure west of Southern South America for 1200 GMT 8 April 1981. Analysis (a) is the operational analysis; it rejected the mean sea level report of ship GWAN (1011 mb). Analysis (b) is a test, which accepted that report. Data dense areas have been shaded.

12 GMT 10 April 1981 Operational Analysis



48 h Forecast from 8 April 1981

Operational



Test

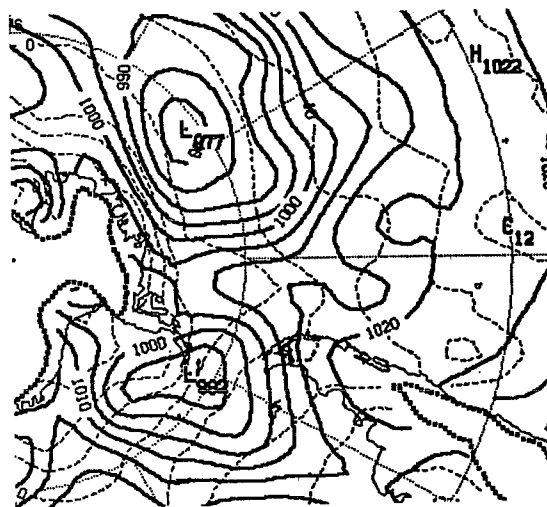
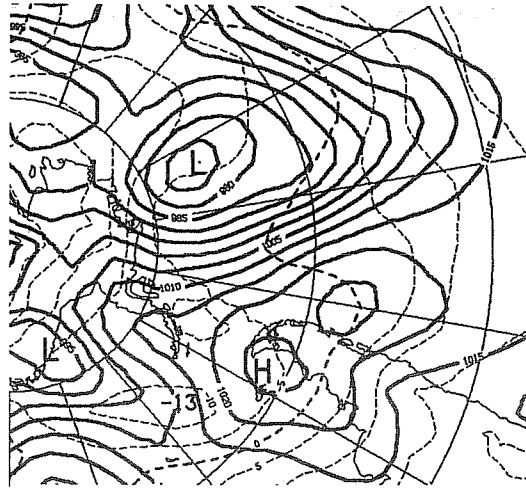


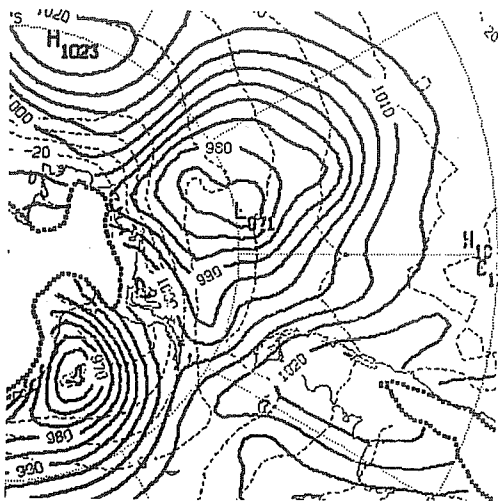
Fig. 4 The 48-hour forecasts from the analyses of Fig. 3 with the verifying analysis (ignore dashed lines).

12 GMT 12 April 1981 Operational Analysis



96 h Forecast from 8 April 1981

Operational



Test

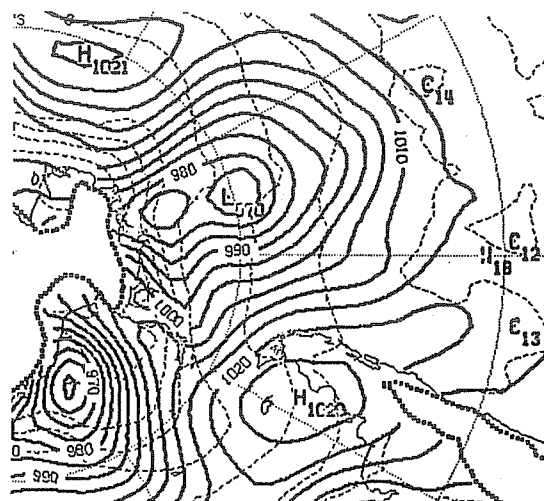


Fig. 5 The 96-hour forecast from the analyses of Fig. 3 with the verifying analysis (ignore dashed lines).

Appendix A), and the analysis calculates height on pressure levels, a vertical interpolation, together with an integration of the hydrostatic equation is required. After the analysis, the reverse interpolation to sigma levels is done. There is a large difference in resolution in the stratosphere between the two coordinate systems (1 sigma and 3 pressure levels above 50 mbar). The interpolation formulae to be used in the stratosphere are not defined by physical considerations, but changing from one formula to another produces widely different analyses. An example of this will be given below.

Apart from mass and wind fields, the model needs an initial prescription of some other data as well. They are also provided by the analysis scheme. Examples to indicate the importance of an accurate analysis of some of these parameters are also provided, namely of humidity and soil moisture.

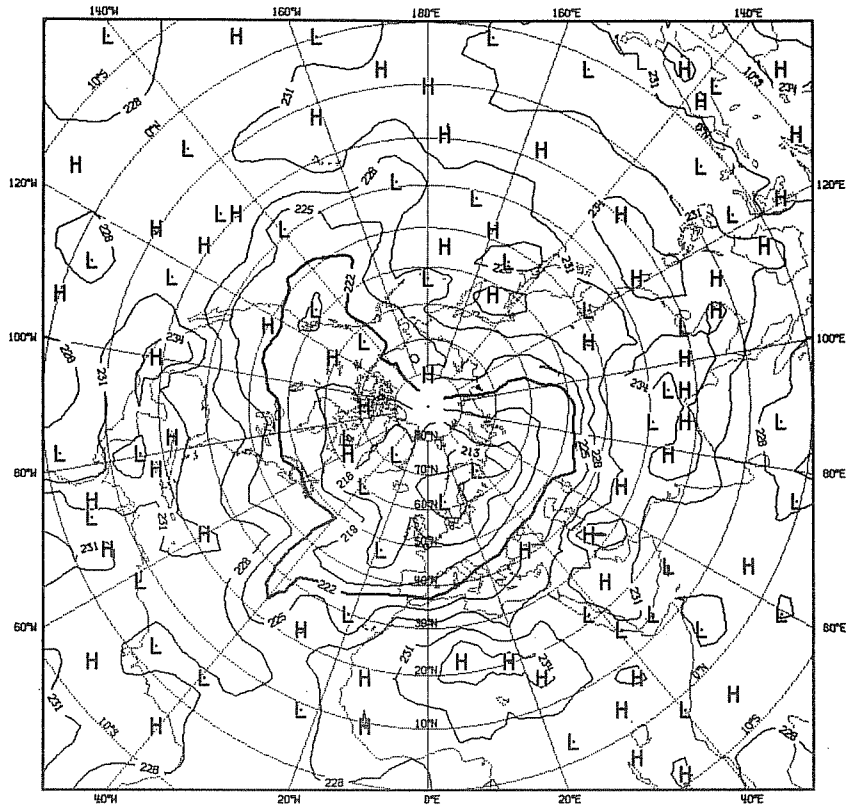
After the analysis, the mass and wind fields are initialized. The last step in a data assimilation cycle is a six-hour forecast to produce the first guess fields for the next analysis. These steps will not be treated here, apart from the remark that a small change in each step may lead to a small change in the first guess, therefore to different data rejection and large changes in the analysis.

3.2 Vertical interpolation

Recently both the sigma to pressure interpolation and the pressure to sigma interpolation have been changed in the ECMWF operational forecasting. The combined effect of these two changes is illustrated in Fig. 6.

The 1 day forecast, as shown in Fig. 7a has been made from an analysis in which the sigma to pressure interpolation of geopotential height was carried out assuming the height to have a functional form of a cubic spline in $\ln p$.

$T_{\sigma} = 0.025$ Operational Analysis



$T_{\sigma} = 0.025$ Test Analysis

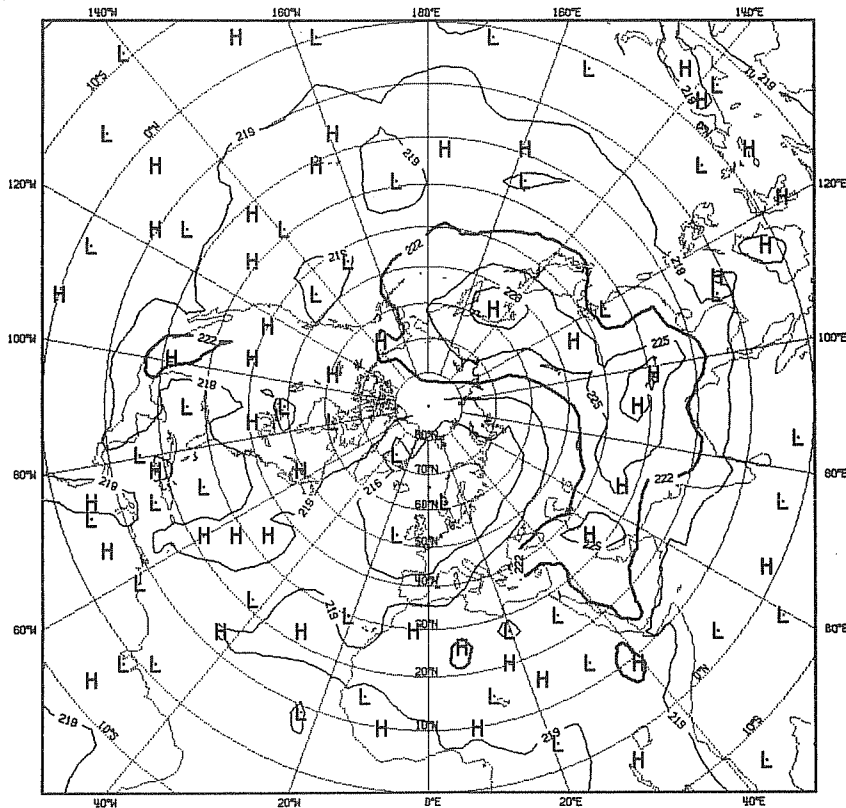
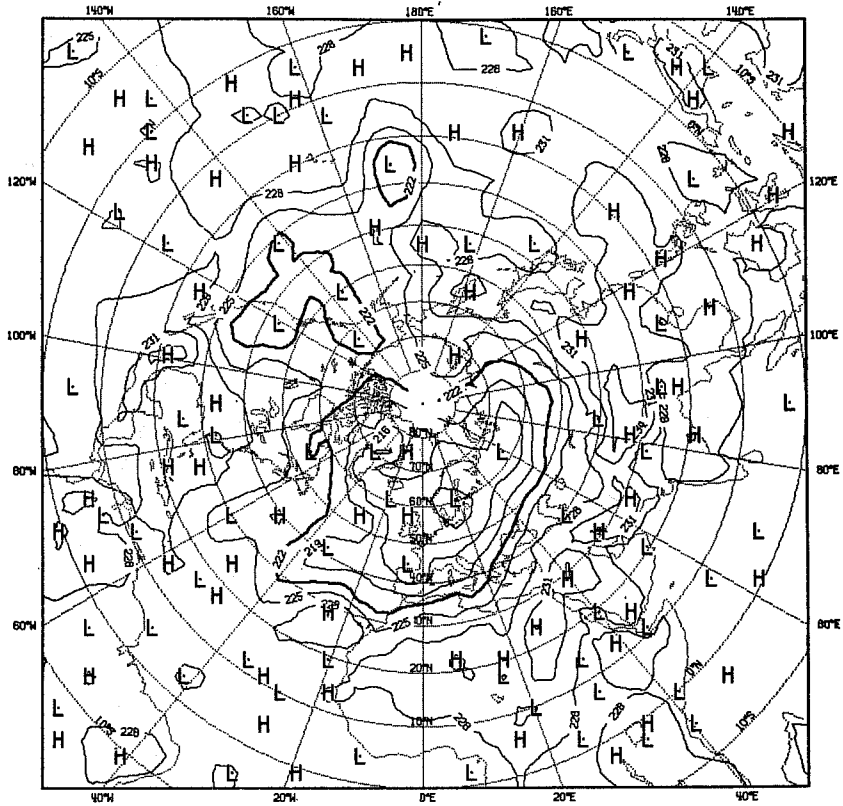


Fig. 6 Top σ -level temperature analysis (K) over the northern hemisphere for 8 April 181, 12 GMT. Top: operational analysis. Bottom: different pressure to sigma coordinates interpolation.

$T_{\sigma} = 0.025$ Operational 24 h Forecast



$T_{\sigma} = 0.025$ Test 24 h Forecast

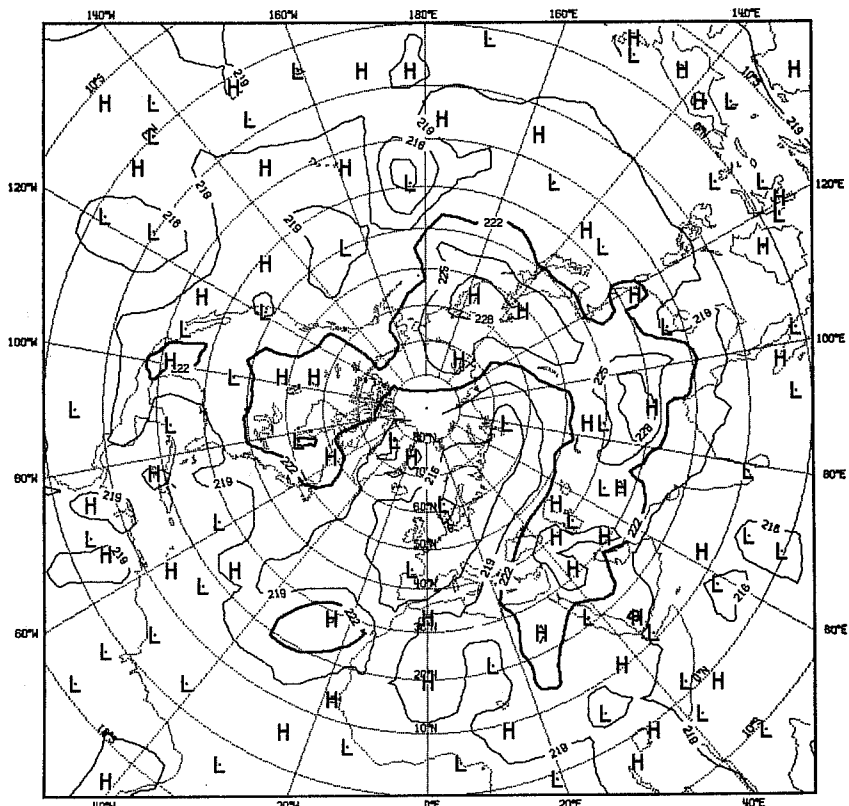


Fig. 7 24-hour forecasts from the analyses of Fig. 6 (units: K).

The reverse interpolation used a volume weighted mean temperature, in accordance with the hydrostatic equation. The forecast as shown in Fig. 7b, however, followed a data assimilation run of 5 cycles of analyses in which the sigma to pressure interpolation was done with an isothermal atmosphere above $\sigma = 0.050$, and the reverse interpolation used a mass weighted temperature mean, which is more consistent with the radiation scheme in use at ECMWF. Both changes reduce the stratospheric tropical temperatures by a few kelvins. The combined effect after 5 assimilation cycles is up to 15K, and the 30 mbar heights after a 24 hour forecast differ by 200 m in places. Also, the noise level in Figs.6b and 7b is much less than that in Figs.6a and 7a.

This example indicates a sensitivity of the analysis and forecast to some parameters in the data assimilation scheme. There are no indications that those parameters exert influence in the troposphere within 10 days, therefore medium range weather forecasting is not necessarily sensitive to them. Quite different is the situation in the troposphere. The vertical interpolation scheme defines static stability and boundary layer structure. It is suspected that the vertical interpolation is a primary source for a sensitivity noted in the ECMWF model, (see Section 4.2). Furthermore, tropical rainfall forecasts have been found sensitive to the formulation of the vertical interpolation of humidity.

3.3 Humidity analysis

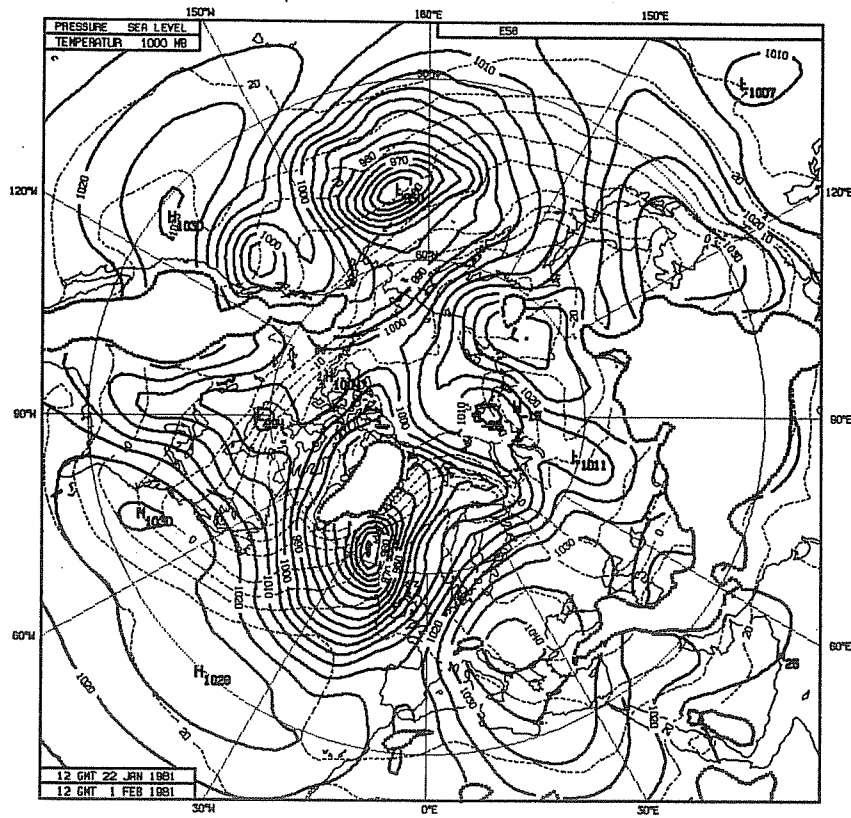
To investigate the sensitivity of the model to the humidity analysis, that analysis has been replaced by the first guess field in an experiment over 5 assimilation cycles. It might be expected that the model would generate its own extratropical humidity field from the initial dynamics within a day or so (Smagorinsky et al, 1970). Therefore the first guess field should be reasonably good. The quality of the observations is, on the other hand, rather low, so that the ECMWF humidity analysis does not differ markedly from

the first guess field. This, but mainly the dynamical generation of the humidity fields explains why in the extratropics little sensitivity to the humidity analysis is found. As shown in Fig. 8, after a 10 day forecast, when also the tropical analysis and forecast play a role in the extratropics, there is still not much change in the extratropical surface fields. This indicates that in this case the humidity analysis is not a parameter that the forecast is sensitive to in the medium range. The humidity analysis, however, changes the global precipitation during the first 24 hours of the experiment's forecast by 10%. It is not ruled out that in other meteorological situations such a change may alter the subsequent forecast much more. Furthermore, the shown case is a northern hemisphere winter case. In summer, with, in general, higher moisture contents and more convective motion, the effect of the humidity analysis may be more pronounced.

3.4 Surface soil moisture analysis

The present ECMWF surface soil moisture analysis consists of replacing soil moisture by its climatology after every analysis. A problem, of course, is, that even that climatology is not reliably known yet. Up to now there are no indications that the extratropical forecast is sensitive to the precise specification of the initial surface soil moisture. But, as shown in Fig. 9, over the Indian Ocean forecast 850 mbar winds changed considerably after a change in soil moisture specification. The forecast shown in Fig. 9a started from a surface soil moisture analysis that was erroneously wet over Southern Arabia. Neither the northward shift of the jet south of Arabia nor the strong inflow into that jet from North Africa in that "wet" forecast are as observed.

10 Day Forecast from Humidity Analysis



10 Day Forecast from Humidity First-Guess

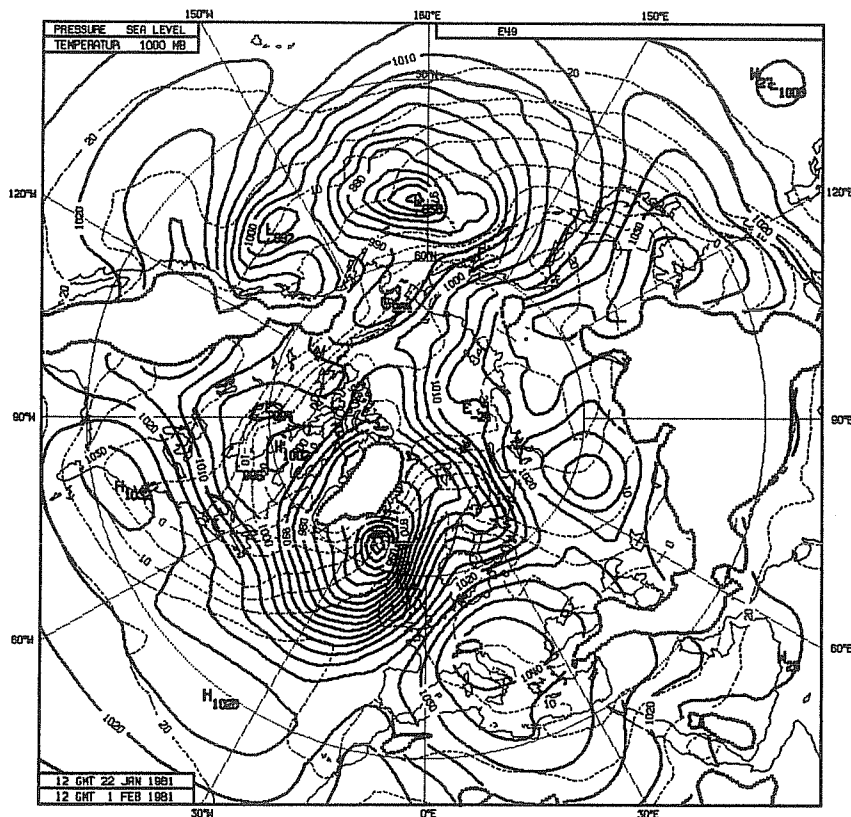


Fig. 8 Two 10-day forecasts from 22 January 1981, 12 GMT. Top: with; Bottom: without humidity analysis. Shown is northern hemisphere mean sea level pressure (mb, full lines) and 1000mb temperature ($^{\circ}$ C, dashed lines).

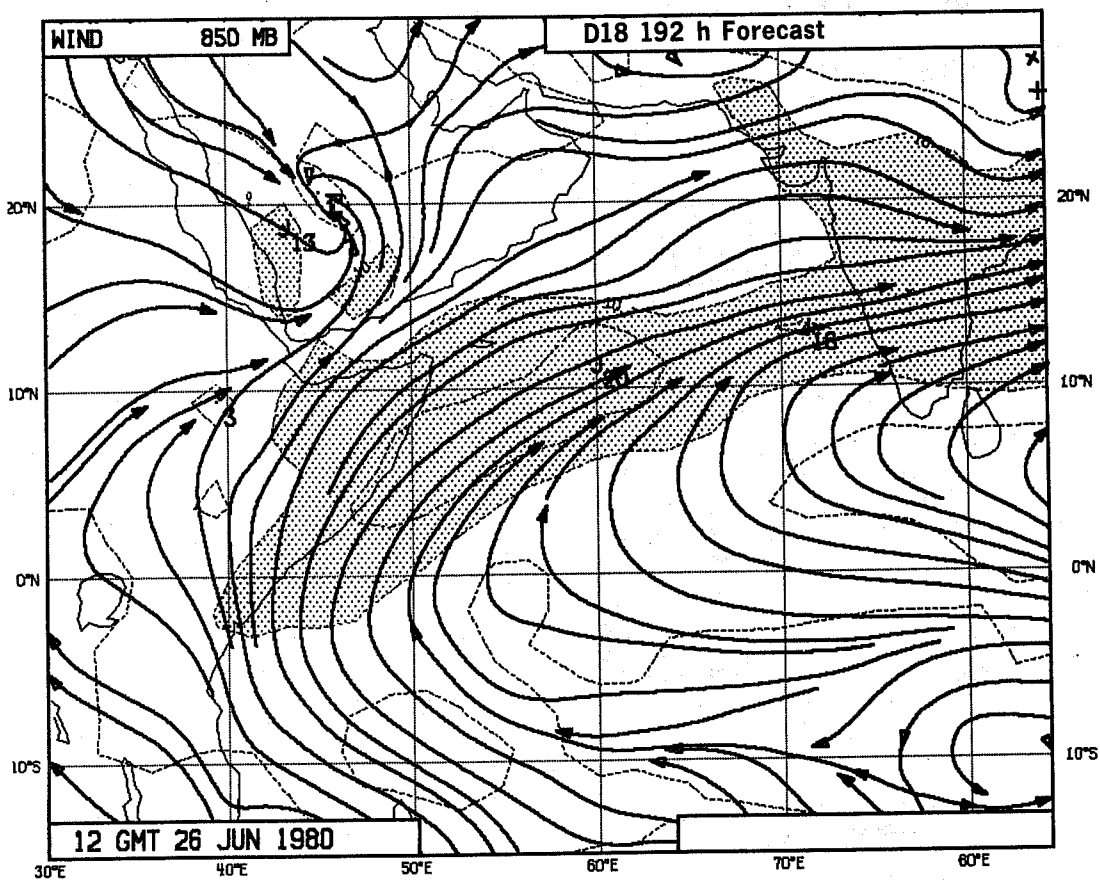
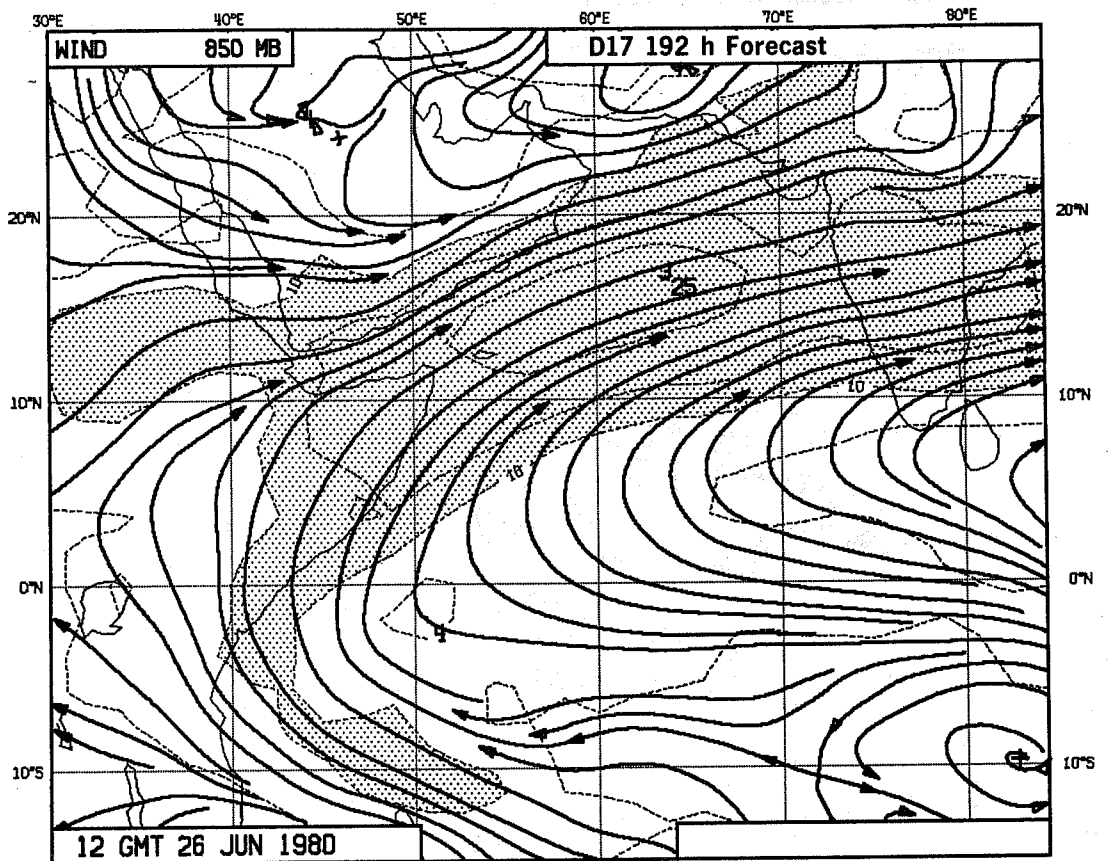


Fig. 9 Two 8-day forecasts of tropical 850mb winds starting from analyses with different soil moisture specification. Numbers in m/s. Shaded are areas with wind speeds in excess of 10 m/s.

4. SENSITIVITY OF THE FORECAST TO THE ANALYSIS

4.1 Introduction

In this section two examples will be presented to indicate that in some synoptic situations the forecast is extremely sensitive to the analysis. The first case concerns the prediction of the "President's-day storm" (February 1979). This example makes it clear that the ECMWF data assimilation scheme may excite unstable waves in the extratropics. The second example shows that a similar phenomenon may also occur in the tropics; the case presented is the four day forecast of the development of hurricane Orchid (September 1980).

In the second section of this paper two cases demonstrated that the analysis is sometimes sensitive to the data checking. For both cases two analyses were carried out, that only differed in the rejection/acceptance of the data that the second section focused upon. The analyses were followed by 10-day forecasts, and the development of the initial difference through the forecasts will be treated in the fourth subsection.

4.2 The President's day storm.

For one of the observation systems experiments performed by the FGGE-group at ECMWF (N.Gustafsson and J.Pailleux, 1981) two 4-day forecasts were made from 17 February 1979, 1200 GMT. One of the forecasts (label F37, Figs. 10,11 and 12) followed an analysis in a data assimilation experiment in which no satellite wind data were used, the other forecast (label F36) one that used those observations. The development of the difference between the two 500 mbar height analysis is shown in the figures. The analyses differ by at most 12 m (west of Mexico), but after four days the difference has amplified to 91 m. The surface pressure difference (Fig. 12b) at the position of the "President's-day storm" (40°N,50°W) is then 24 mbar. Quite predictably, in such a sensitive situation, neither forecast is very good. Both underpredict the development of the low pressure system.

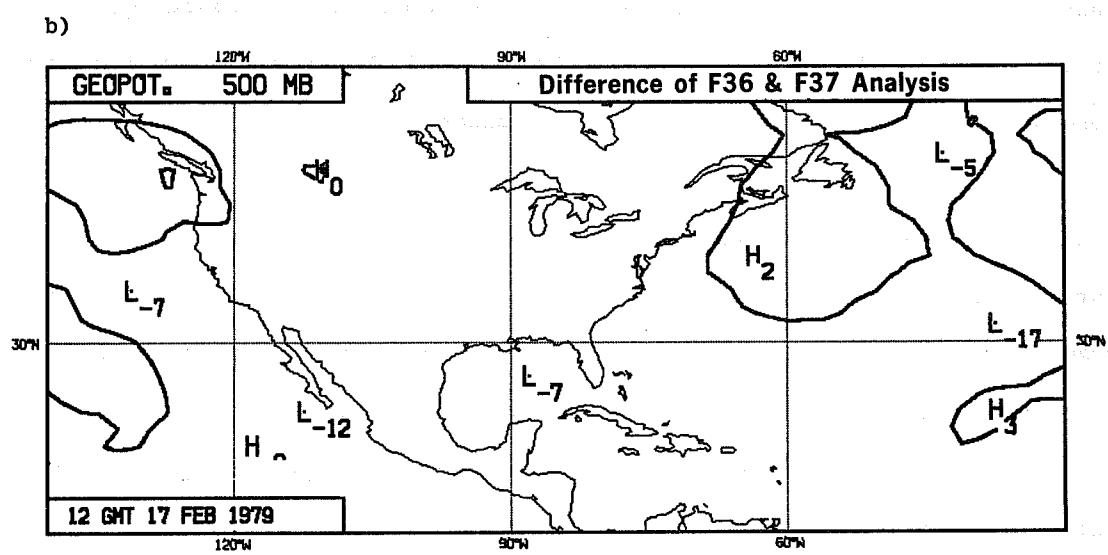
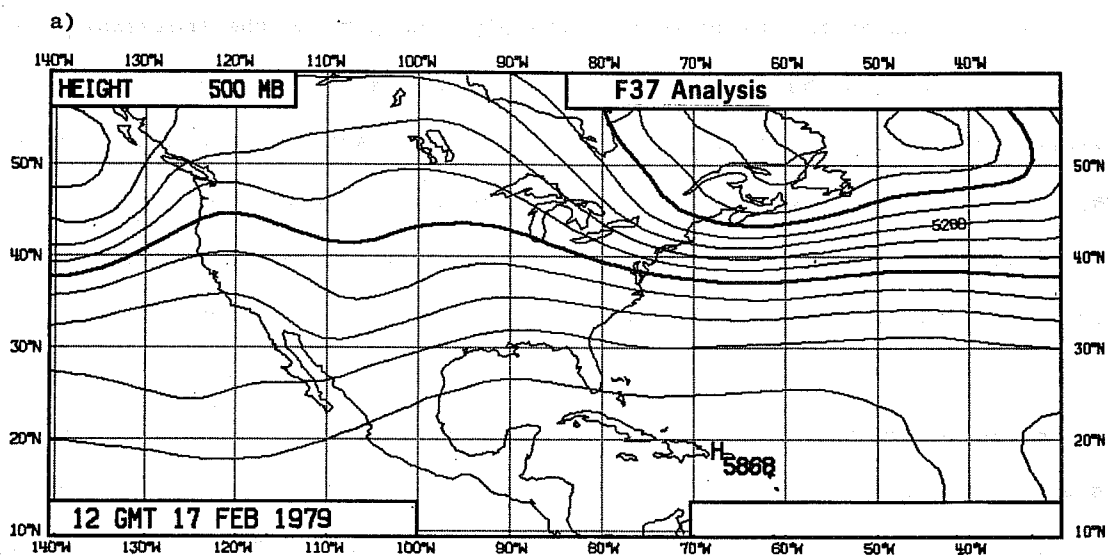
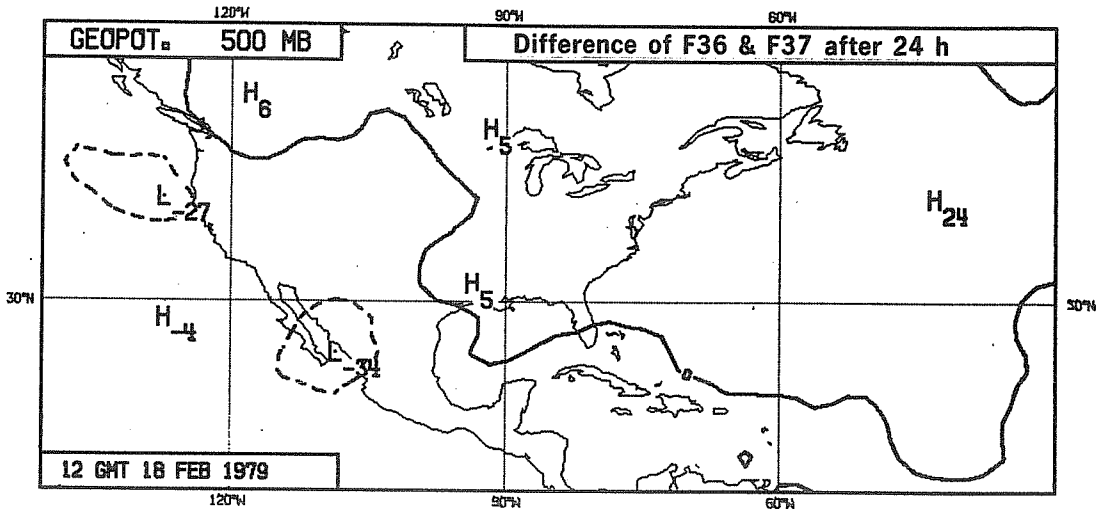


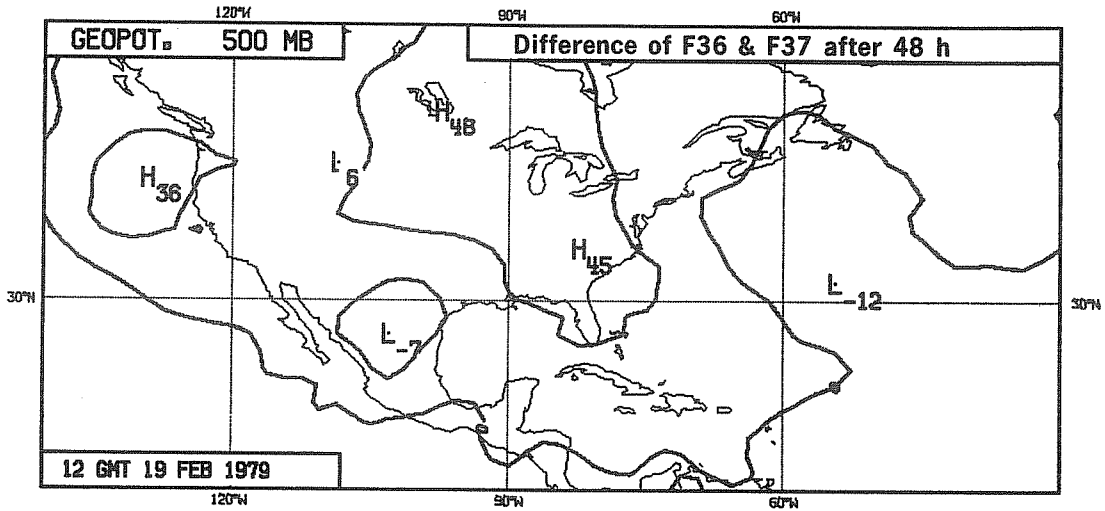
Fig. 10(a) 500mb height analysis (F37) for 12 GMT 17 February 1979. In this analysis no satellite wind observations were used.

(b) Difference of analysis (F36), in which those observations were used, with the analysis shown in (a). Numbers in m.

a)



b)



c)

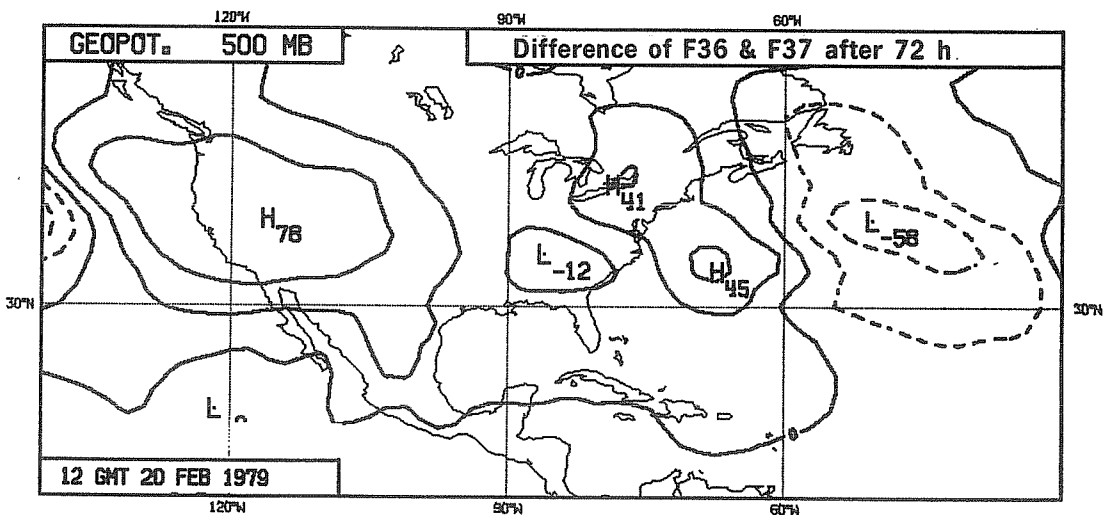


Fig. 11 Difference of 500mb geopotential height between the forecasts made from the analyses of Fig. 10 after 24h (a), 48h (b) and 72h (c). Numbers in m. Contours for strictly negative values have been dashed.

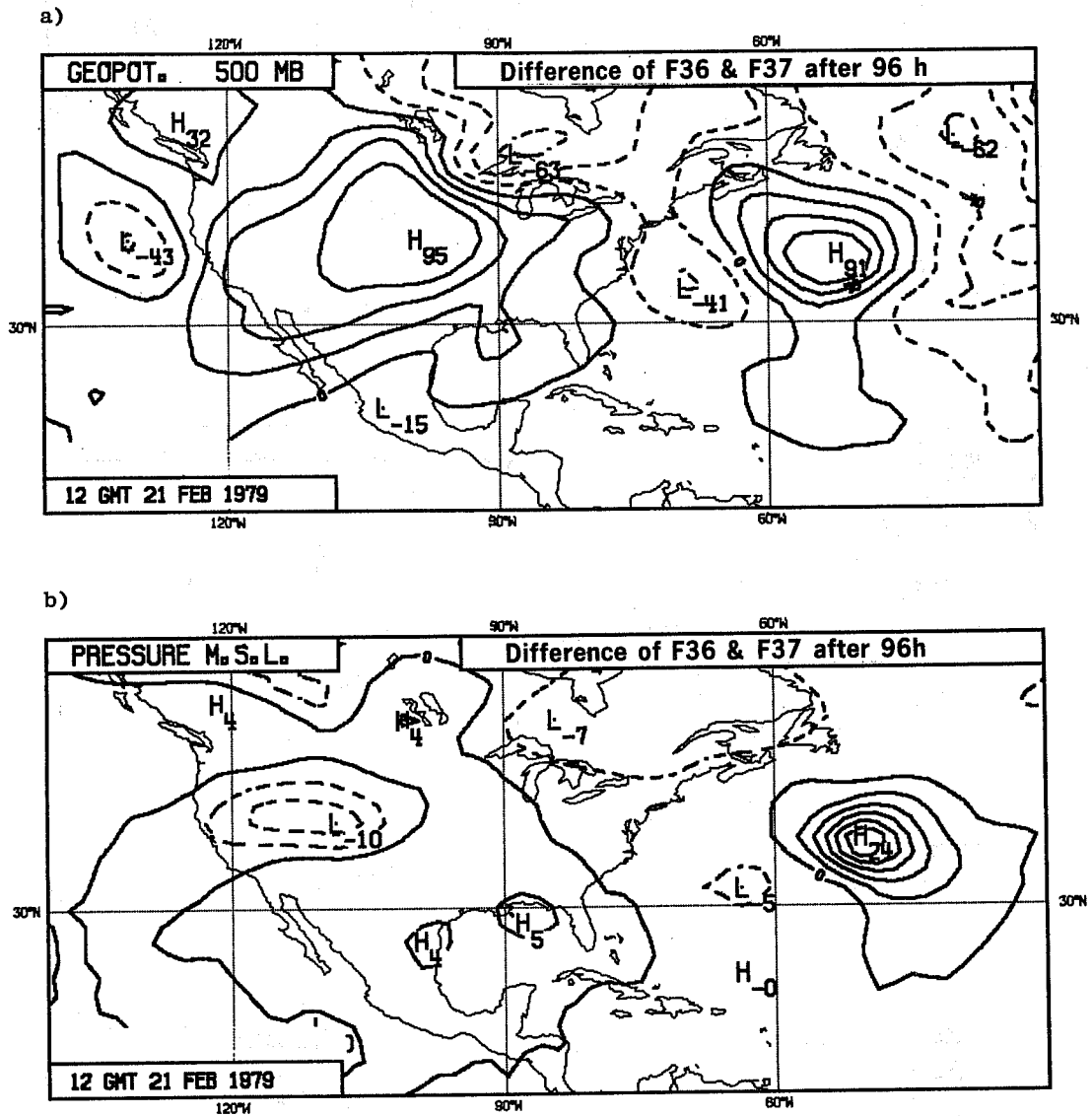


Fig. 12 Difference of 500mb geopotential height (m) (a), and mean sea level pressure (mb) (b), between the forecasts made from the analyses of Fig. 10 after 96 hours. Strictly negative contours have been dashed.

Gustafsson and Pailleux relate the explosive growth of the original difference to the vertical interpolation between pressure and sigma coordinates. The vertical interpolation interacted with cloud parameterization and radiative cooling in the model to produce different static stabilities in the two analyses. It was this change in static stability rather than the change in height fields that the forecast sensitivity originated from.

4.3 Hurricane Orchid

Originally in the ECMWF data assimilation scheme no correct distinction was made between real and virtual temperature when using the hydrostatic equation to transform the analysed variable height to the model variable temperature. In general the difference between the two temperatures is small, except in the humid tropical boundary layer, which plays a crucial role in the development of tropical hurricanes. Indeed, after the correction of the treatment of real and virtual temperatures, the hurricane Orchid was well predicted in a four day forecast from 4 September 1980, 1200 GMT (Fig. 13a), whereas it was hardly seen in the original forecast (Fig. 13b). The ECMWF verifying analysis is shown in Fig. 13c. This analysis has been obtained in a data assimilation run that included the analysis of Fig. 1c, 24 hours earlier. Had at that time the EREBO TEMP report been used (as in Fig. 1b) instead of the SYNOP report, the analysis at 8 September 1200 GMT would have shown a centre pressure of 998 mbar. (This indicates that even the verifying analyses are sensitive to certain parameters....). Independent reports suggest that the centre pressure was 985 mbar on 8 September, 1200 GMT.

4.4 Development of initial disturbances through the 10-day forecast

For the 7 September 1980, 1200 GMT, two analyses were made, one using the TEMP report from the ship with call sign EREBO (Fig. 1b) and one using the SHIP report (Fig. 1c) for the 1000 mbar height. The two analyses were the same in all other respects. A similar procedure was followed for 8 April

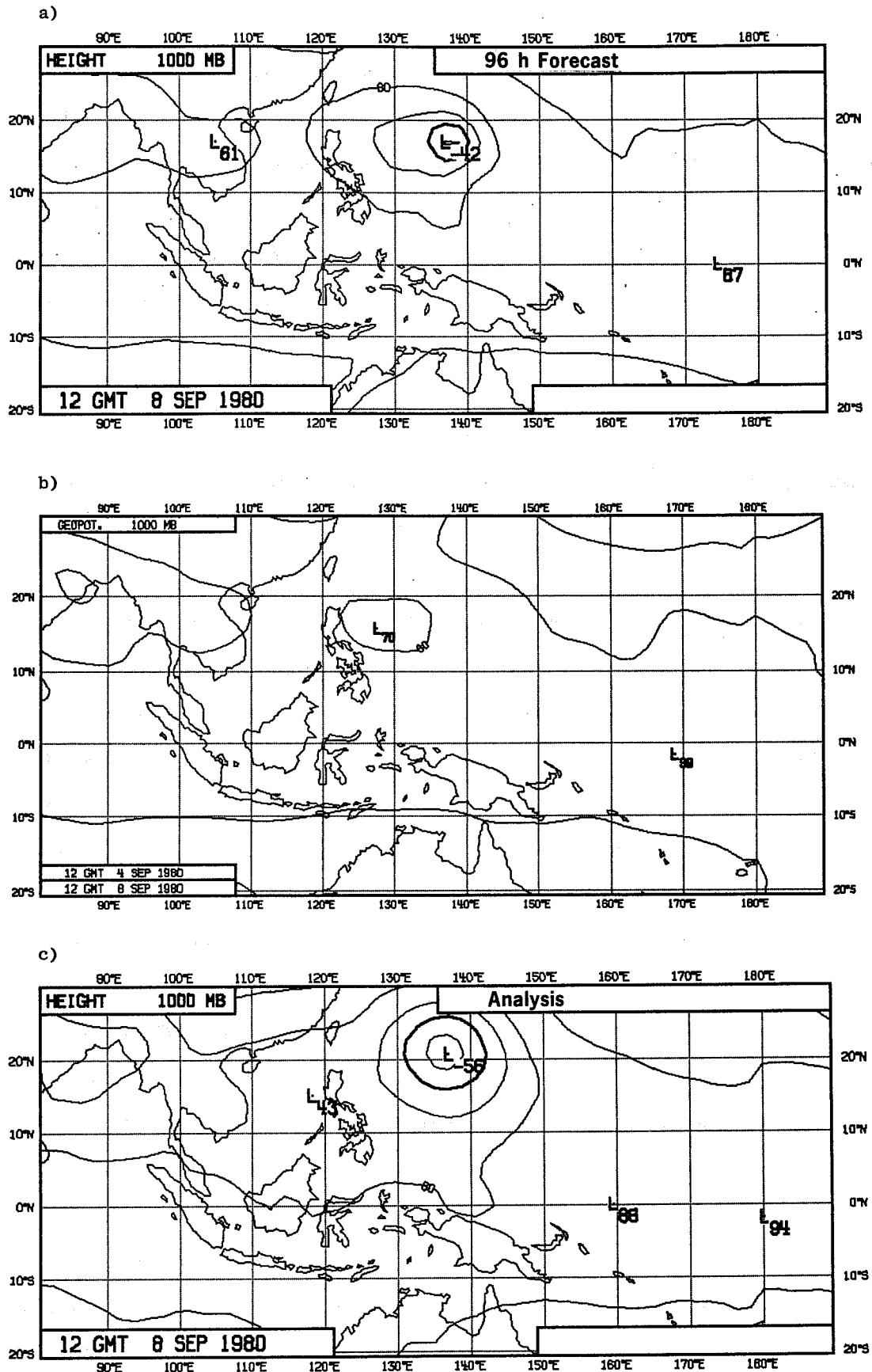


Fig. 13 Two four-day forecasts of hurricane Orchid valid for 12 GMT 8 September 1980.

- a) Correct treatment of humidity in the hydrostatic equation.
 - b) Use of real instead of virtual temperature in the hydrostatic equation.
 - c) Verifying analysis.
- Contour interval is 40 m.

1981, 1200 GMT, the only difference between the two analyses now being the treatment of the surface pressure report of the ship with call sign GWAN (Fig. 3).

The difference between two corresponding analyses can be considered as an initial perturbation. The growth of that perturbation during a 10-day forecast was studied by running forecasts from each analysis. Some properties of the perturbation are illustrated in Figs. 14 through 19 and in Table 1.

The disturbance survives initialization with a 1 mbar amplitude reduction in surface pressure (Table 1). With the used sign convention the maximum disturbance is positive. The optimum interpolation method has the property to introduce negative lobes if other observations indicate the presence of gradients. This effect is seen for horizontal gradients in Fig. 15 and for vertical gradients in Table 1. The initial perturbation develops into a propagating and growing wavetrain (Figs. 14 and 15). There is a strong resemblance with figures shown by Simmons and Hoskins (1979). Other properties of the wavetrains correspond to their results as well, e.g. the zonal velocity of the forward fringe of the wavetrain is roughly 60% of the zonal wind speed at 200 mbar; new waves develop near the position of the initial disturbance; the systems have a vertical phase tilt; the trailing wave grows faster aloft than near the ground..

Simmons and Hoskins found also that the disturbance first required a few days before it really started to grow. Something similar is present in the 8 April 1981 case, but cannot be identified in the hurricane case. Fig. 16 shows the growth rate of several error measures. The standard deviation between the geopotential heights in the two corresponding forecasts has been evaluated over the 1000 to 200 mbar standard pressure levels and over the

Table 1. Some properties of the perturbations in the initial conditions for the two studied cases.

| | 7 September 1980 (case: EREBO) | 8 April 1981 case: GWAN) |
|------------------|---------------------------------------|-----------------------------|
| Sign convention: | Positive is: accept TEMP, reject SHIP | accept SHIP |

Max. difference in analyses:

| | | |
|-----------------------------------|----|----|
| surface pressure (mbar) | | |
| before initialization: | 4 | 12 |
| after initialization: | 3 | 11 |
| 500 mb height, after initial.(m): | -4 | 56 |

Table 2. Precipitation from convective cloud, accumulated from the start of the forecast and surface pressure in the centre of hurricane Orchid in the 7 September 1980 case.

| Analysis uses EREBO report: TEMP (998 mbar) | SHIP (992 mbar) | | | |
|---|-----------------|--------|-------------|--------|
| | CONV. PREC. | MSLP | | |
| Time since forecast start (days) | (mm) | (mbar) | CONV. PREC. | MSLP |
| | | | (mm) | (mbar) |
| 0 | 0 | 1000 | 0 | 997 |
| 1 | 62 | 1001 | 92 | 997 |
| 2 | 82 | 1000 | 141 | 996 |
| 3 | 134 | 1001 | 253 | 997 |
| 4 | 176 | 998 | 255 | 993 |

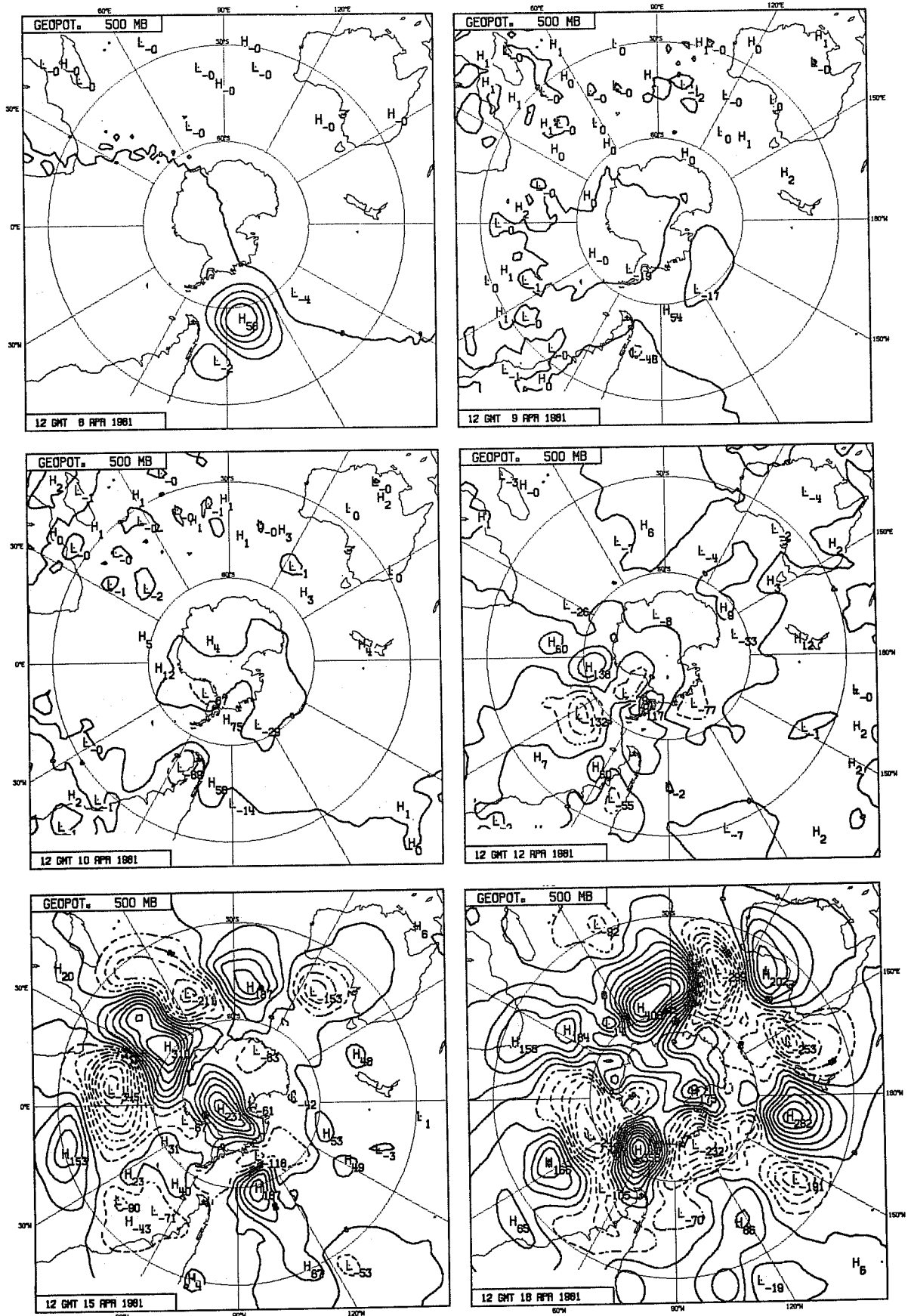


Fig. 15 As Fig. 14 for the southern hemisphere, initial date is 8 April 1981. The contour interval in the top left panel ('analysis') is 10 m, elsewhere it is 40 m.

latitude band 20° - $82^{\circ}.5$ (north for 7 September 1980, south for 8 April 1981). The initial perturbation in the hurricane case is to a great extent outside this verification area, so that the initial growth cannot be inferred from this standard deviation. Fig. 16 shows that the maximum amplitude of the hurricane disturbance grows rapidly, also in the early stages, but both forecasts for this case do not develop the hurricane strongly (Table 2). (Phase shifts between the two forecasts account for the amplitude growth of the disturbance). Presumably the initial growth is due to latent heat release rather than baroclinic instability, and therefore the early stages of this case do not behave similarly to those shown by Simmons and Hoskins.

The standard deviation (Fig. 16) grows exponentially over a large range of values, with a doubling time of less than 2 days. This growth rate is the same in the two cases studied and rather independent of wavelength, as is shown by the separate display of the wavenumber groups 1-3 (σ_L) and 4-9 (σ_M). The maximum amplitude of the disturbance grows considerably slower, because this measure does not take the growth of the horizontal and vertical extent of the disturbance into account.

Although in both cases the forecasts differed considerably in the later stages of the forecast, the synoptic patterns were very much the same in the first four (8 April 1981) or six (7 September 1980) days (Figs. 17 and 18). For both cases holds that in that stage of the forecast the anomaly correlation coefficient between the two forecasts, evaluated over the same area as the standard deviation in Fig. 16, starts coming down (Fig. 19). Furthermore, the two forecasts from 7 September 1980 crossed the 60% anomaly correlation with ECMWF analyses at day 6, and those from 8 April 1981 at day 4. All these measures suggest that the atmosphere was predictable in the relevant hemisphere up to day 4 in the southern and up to day 6 in the northern hemisphere case.

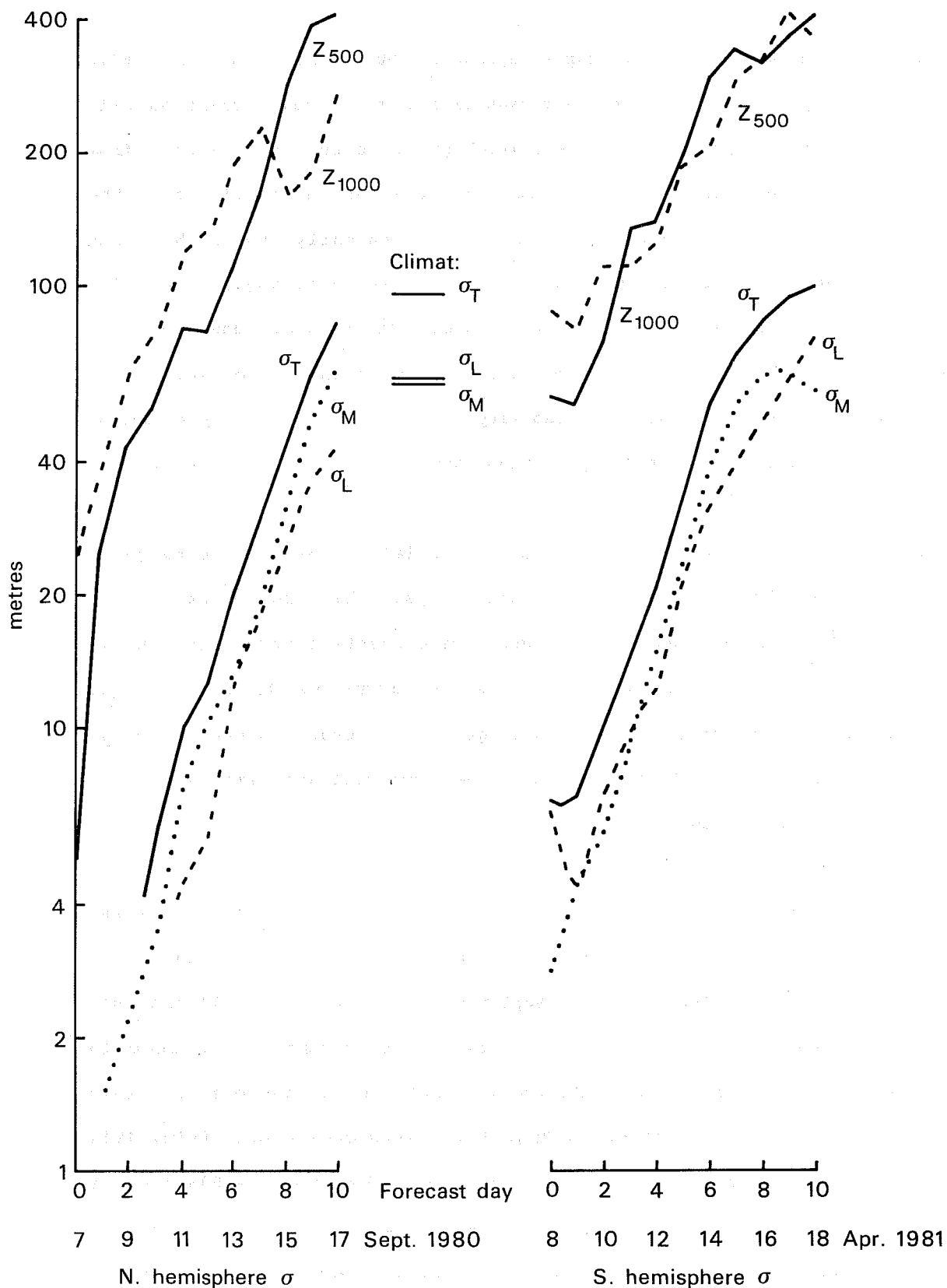


Fig. 16 Maximum amplitude of 1000 (Z_{1000}) and 500 mb height (Z_{500}) difference between the forecast pairs from 7 September 1980 and from 8 April 1981; and standard deviation of height difference between the forecasts over 20° - 82.5° N and S respectively and 1000-200 mb in the zonal wave-number bands: total (σ_T), 1-3 (σ_L) and 4-9 (σ_M). Also indicated is the September climatological standard deviation for the area 20° - 82.5° N, 1000-200 mb in the same zonal wavenumber bands.

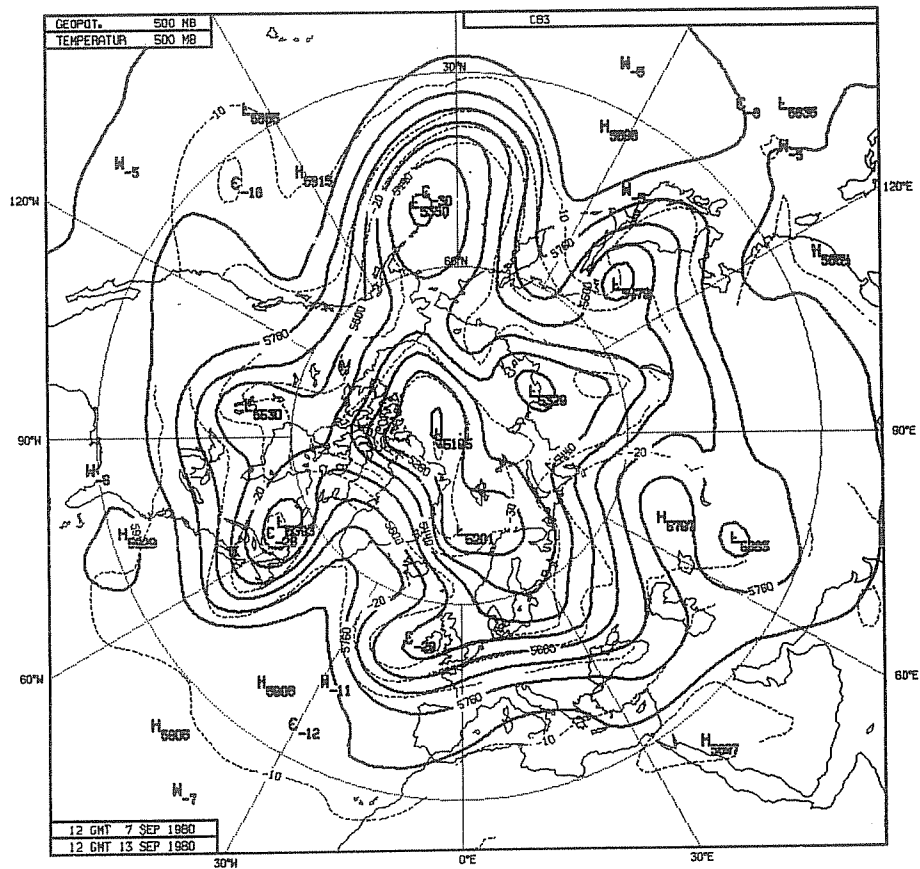
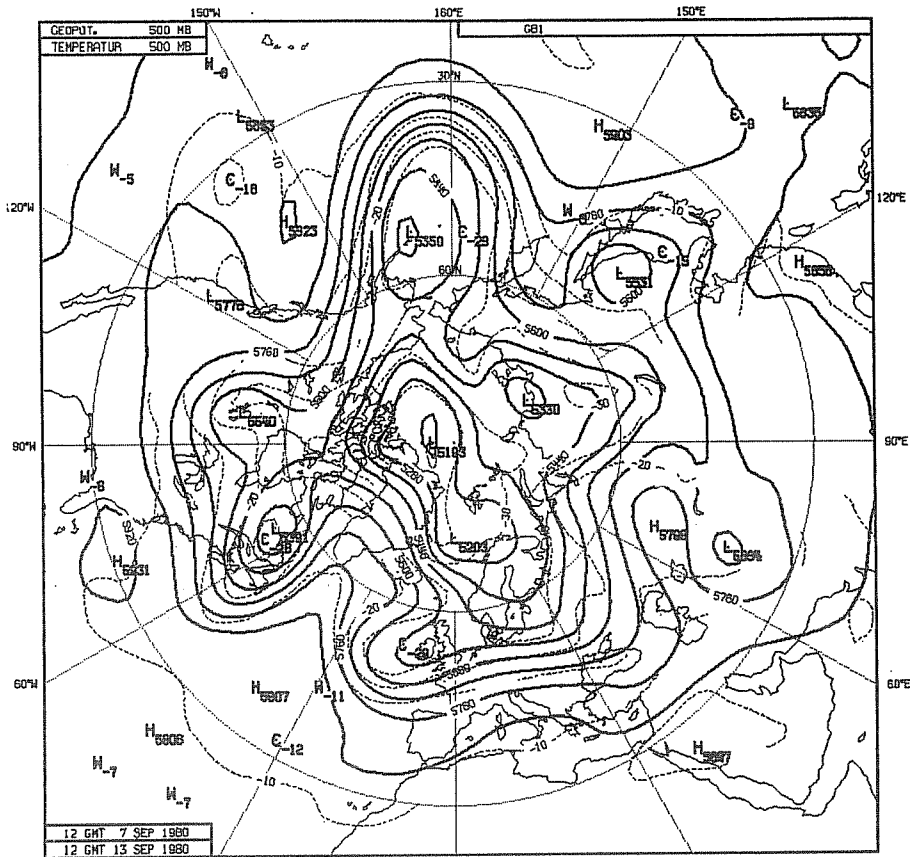


Fig. 17 Northern hemisphere 500 mb height (m, full lines) and temperature ($^{\circ}\text{C}$, dashed lines) at day 6 in the two forecasts from 7 September 1980.

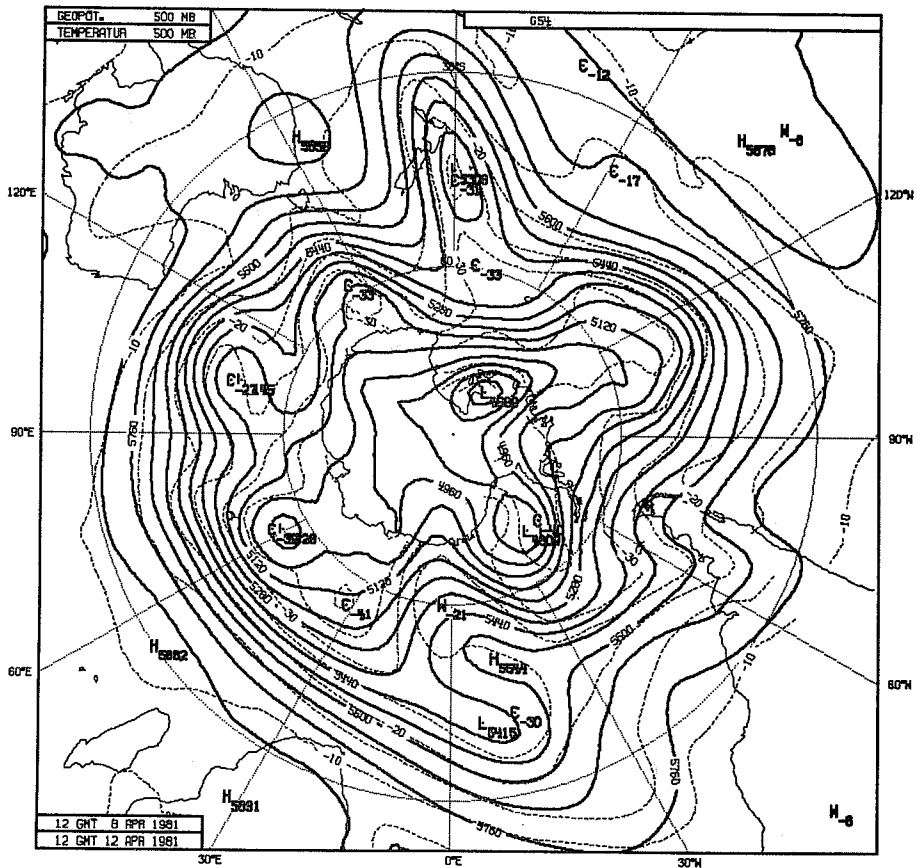
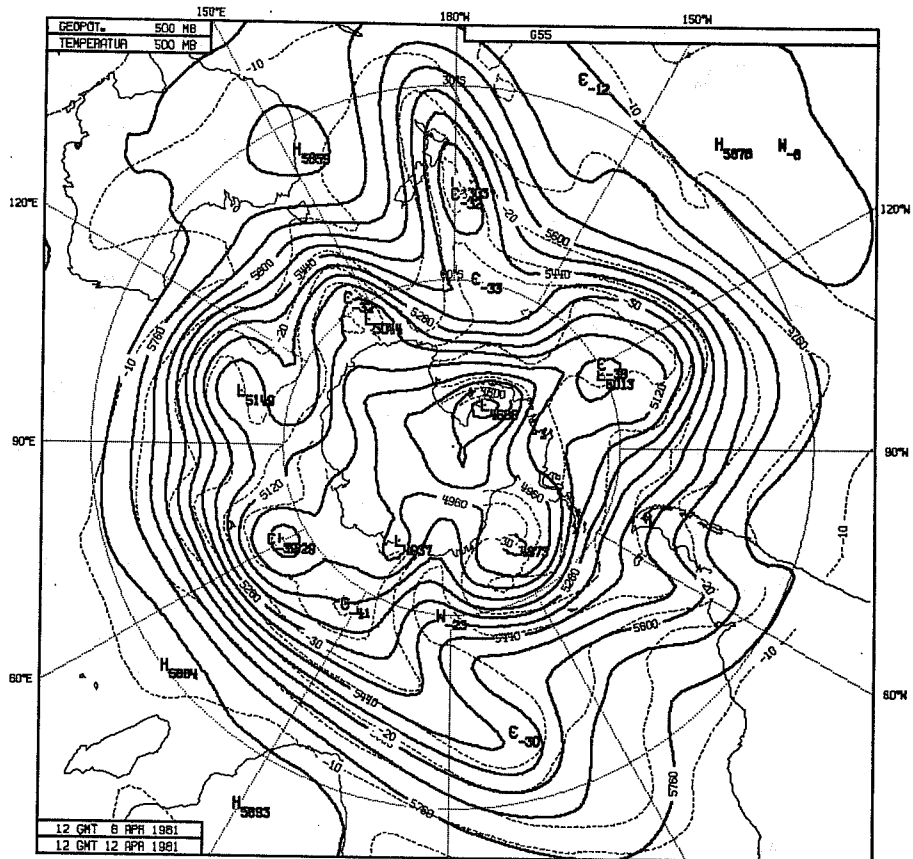


Fig. 18 Southern hemisphere 500 mb height (m, full lines) and temperature ($^{\circ}\text{C}$, dashed lines) at day 4 in the two forecasts from 8 April 1981.

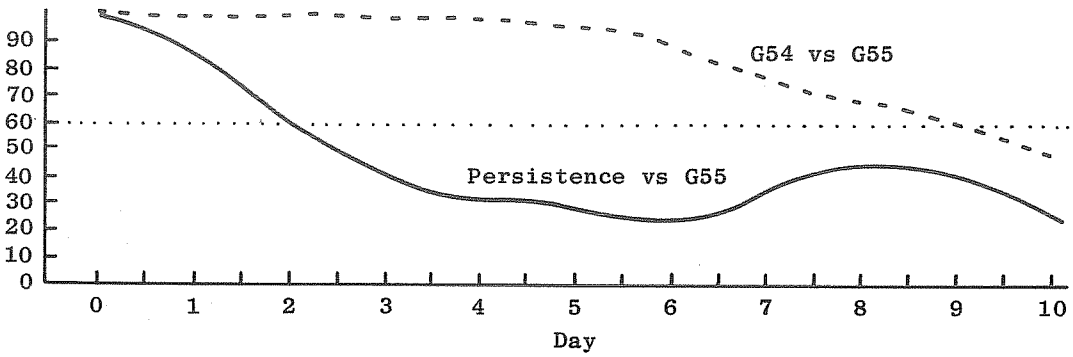
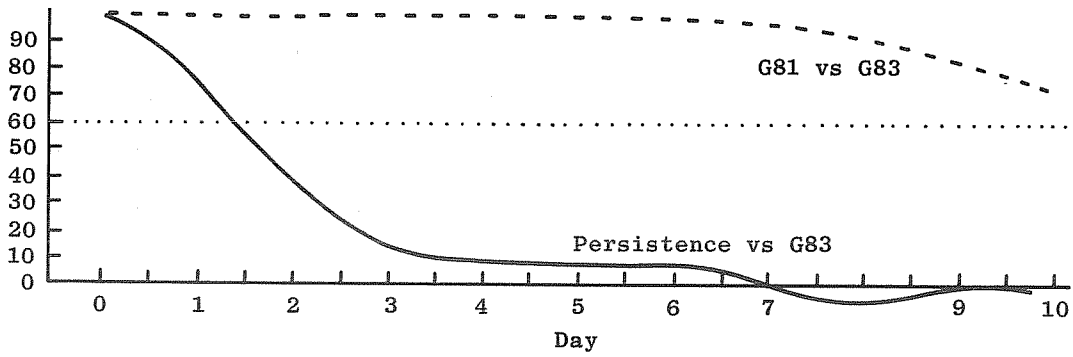


Fig. 19 Anomaly correlation of height over 20° - 82.5° , 1000-200 mb, between the two forecasts from 7 September 1980 (top, Northern Hemisphere) and those from 8 April 1981 (bottom, Southern Hemisphere). Heavy lines show the correlation of persistence with one of the forecasts.

In both cases the anomaly correlation between the two forecasts started only to deviate visibly from 1 by the time that the anomaly correlation between forecast and analysis went below 60%. An attempt has been made to obtain some feeling of how much of the more rapid decline of the latter correlation is due to the combined effect of initial errors and how much to forecast model errors. (Appendix B). A large number (estimates vary from twenty to forty, depending on the very tentative assumptions) of errors in the initial state of similar amplitude and growth rate would be required to decrease the 4 respectively 6 day correlation between two corresponding forecasts to that between a forecast and the verifying analysis, if it is assumed that the effects of the initial errors are uncorrelated and that the growth rate is the same for all initial errors. It is unlikely that the initial state contains so many large errors. There are of course many more much smaller errors, but every halving of initial amplitude requires a quadrupling of number of errors to produce the same effect. This suggests that the errors introduced at the beginning of the model integration do, by far, not account for the errors at the end of the integration, so that also errors must have been introduced during the integration. It is stressed, however, that the assumptions made to arrive at this conclusion are not necessarily correct due to the nonlinearity of the atmosphere and the model. A more quantitative estimate of these model errors relative to the analysis errors needs, but also warrants, a deeper investigation.

Monte-Carlo type experiments with perturbations of the initial conditions suffered up to now from some problems. It has been difficult to make the initial disturbances survive initialization (Hollingsworth, 1979), but it appears that the cases presented here have overcome this problem. Another problem is the computational expense of Monte-Carlo experiments with a full model. If there is indeed sufficient similarity with the experiments of Simmons and Hoskins, a far cheaper model may be useable.

CONCLUSIONS AND OUTLOOK

At ECMWF, both during operational and experimental work, many cases have been encountered where the produced analysis and/or forecasts were very sensitive to certain parameters within the analysis scheme. Mostly the sensitivities are produced by discontinuities during data checking, but also the excitation of unstable waves plays a role occasionally. The exact correct value of many of the relevant parameters is not known yet; much of the work in the ECMWF analysis section is devoted to identifying and determining those parameters. Many problems, however, are due to inconsistencies or insufficiencies in the available observation systems. There is no hope that these problems will be solved in the near future. The presented examples show that the quality of a medium range weather forecast may depend strongly on the quality of the initial analysis. With the present observational systems one should not expect that it is possible to produce such a forecast with a constant, high quality. Only the average quality might be increased with suitable tuning of the data assimilation scheme.

The study of the development of an initial perturbation through a model integration may increase insight in the relative merits of a good analysis and a good model for medium range weather forecasting, and identify areas of atmospheric instability. A promising way of introducing the initial perturbation is by changing the quality control of one observational datum. The development of such an initial perturbation in the complicated ECMWF model resembles that found in far simpler models.

Acknowledgement

The presented examples have been taken from experiments with the ECMWF data assimilation scheme. Most of the experiments have been run by others, and I am indebted to them for allowing me to use their results. I would like to thank particularly the members of the data assimilation group (J. Anderson, P. Lonnerberg, D. Shaw, J. Van Maanen and W. Wergen) and of the FGGE group

(N. Gustafsson, P. Kallberg, J. Pailleux and S. Uppala). I also thank
A. Hollingsworth for his very useful suggestions and help.

References

- Gustafsson, N. and J.Pailleux 1981 On the quality of FGGE data and some remarks on the ECMWF data assimilation scheme. ECMWF Technical Memorandum 37, p 29.
- Hollingsworth, A. 1979 An experiment in Monte-Carlo forecasting, In: Proceedings of the ECMWF workshop on Stochastic Dynamic Forecasting, Reading, 17-19 October.
- Lorenc, A. 1981 A global three-dimensional multivariate statistical interpolation scheme. Mon.Wea.Rev., 109, 701-721.
- Simmons, A. and B. Hoskins 1979 The downstream and upstream development of unstable baroclinic waves. J.Atmos.Sci., 36, 1239-1254.
- Smagorinsky, J., K. Miyakoda and R.F. Strickler 1970 The relative importance of variables in initial conditions for dynamical weather prediction. Tellus, 22, 141-157.
- Williamson, D. and C. Temperton 1981 Normal mode initialization for a multi-level grid-point model. Part II: nonlinear aspects. Mon.Wea.Rev., 109, 744-757.

(Horizontal Resolution 1.875° Lat/Lon)

ANALYSIS

ϕ, u, v, q (for $p \geq 300$)

PREDICTION

T, u, v, q

p (mb)

- 10
- 20
- 30
- 50
- 70
- 100
- 150
- 200
- 250
- 300
- 400
- 500
- 700
- 850
- 1000

σ

- 0.025 (σ_1)
- 0.077
- 0.132
- 0.193
- 0.260
- 0.334
- 0.415
- 0.500
- 0.589
- 0.678
- 0.765
- 0.845
- 0.914
- 0.967
- 0.996 (σ_{15})

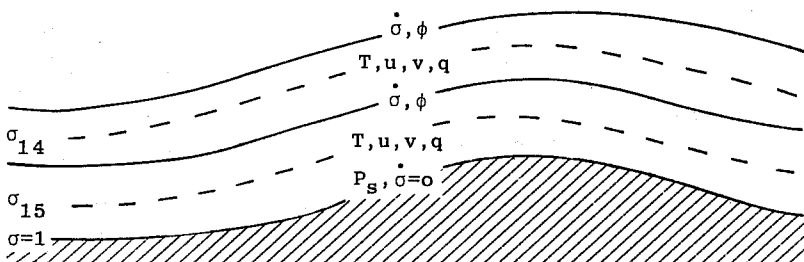
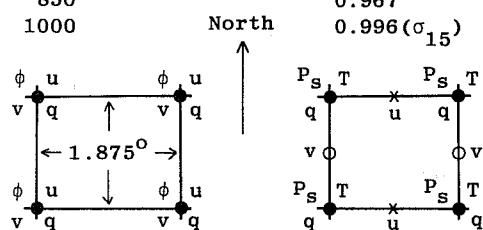
$\sigma=0$

σ_1

$\dot{\sigma}=0$

T, u, v, q

σ, ϕ



Vertical and horizontal (latitude-longitude) grids and dispositions of variables in the analysis (left) and prediction (right) coordinate systems.

ANALYSIS

Method

3 dimensional multi-variate (15-analysis levels, see above)

Independent variables

λ, ϕ, p, t

Dependent variables

ϕ, u, v, q

Grid

Non-staggered, standard pressure levels

First guess

6 hour forecast (complete prediction model)

Data assimilation frequency

6 hour (\pm 3 hour window)

INITIALISATION

Method

Non-linear normal mode, 5 vertical modes, adiabatic

PREDICTION

Independent variables

λ, ϕ, σ, t

Dependent variables

T, u, v, q, p_s

Grid

Staggered in the horizontal (Arakawa C-grid). Uniform horizontal (regular lat/lon). Non-uniform vertical spacing of levels (see above).

Finite difference scheme

Second order accuracy

Time-integration

Leapfrog, semi-implicit ($\Delta t = 15$ min) (time filter $\nu = 0.05$)

Horizontal diffusion

Linear, fourth order (diffusion coefficient = $4.5 \cdot 10^{15} \text{ m}^4 \text{ s}^{-1}$)

Earth surface

Albedo, roughness, soil moisture, snow and ice specified geographically. Albedo, soil moisture and snow time dependent.

Orography

Averaged from high resolution (10') data set

Physical parameterisation

- (i) Boundary eddy fluxes dependent on roughness length and local stability (Monin-Obukov)
- (ii) Free-atmosphere turbulent fluxes dependent on mixing length and Richardson number
- (iii) Kuo convection scheme
- (iv) Full interaction between radiation and clouds
- (v) Full hydrological cycle
- (vi) Computed land temperature, no diurnal cycle
- (vii) Climatological sea-surface temperature

APPENDIX B

EFFECT OF n UNCORRELATED ERRORS ON THE CORRELATION COEFFICIENT

In this Appendix the correlation coefficient between two fields ("forecast" and "analysis") will be calculated if the difference between forecast f and analysis a is the sum of n uncorrelated error fields ϵ_i ($i=1\dots n$):

$$f = a + \sum_{i=1}^n \epsilon_i \quad (B1)$$

$$\begin{aligned} \overline{\epsilon_i \epsilon_j} &= \sigma_i^2 \text{ if } i=j \\ &= 0 \text{ if } i \neq j \end{aligned} \quad (B2)$$

In (B2), σ_i^2 represents the variance of the error ϵ_i , and an overbar is used to denote averaging over the field. The notation $\tau_i = \sqrt{\sigma_i^2 / a^2}$ will be used.

First, it will be assumed that analysis and error fields are uncorrelated:

$$\overline{a \epsilon_i} = 0 \quad (i=1\dots n) \quad (B3)$$

The correlation between forecast and analysis is then

$$c_{fa} = \frac{\overline{af}}{(\overline{a^2} \overline{f^2})^{1/2}} \quad (B4)$$

with, according to (B1) and (B3):

$$\overline{af} = \overline{a^2} \quad (B5)$$

and

$$\overline{f^2} = \overline{a^2} + \sum_{i=1}^n \sigma_i^2 = \overline{a^2} \left(1 + \sum_{i=1}^n \tau_i^2 \right) \quad (B6)$$

So:

$$c_{fa} = \frac{1}{\left(1 + \sum_{i=1}^n \tau_i^2 \right)^{1/2}} \quad (B7)$$

If all error fields have the same variance ($\tau_i^2 = \tau^2$ for all i), this becomes

$$c_{fa} = \frac{1}{(1 + n\tau^2)^{\frac{1}{2}}} \quad (\text{B8})$$

Present forecast models do not increase the variance of the forecast field over that of the analysis field. A simple assumption, to replace (B3), accounts for this, namely:

$$\sum_i \overline{\epsilon_i a} = -\frac{1}{2} \sum_i \overline{\epsilon_i^2} = -\frac{1}{2} \overline{a^2} \sum_i \tau_i^2 \quad (\text{B9})$$

With this correlation between analysis and error fields, (B6) is replaced by

$$\overline{f^2} = \overline{(a + \sum \epsilon_i)^2} = \overline{a^2} \quad (\text{B10})$$

which indicates a constant forecast field variance.

Now (B5) and (B7) are replaced by, respectively

$$\overline{af} = \overline{a^2} - \frac{1}{2} \sum \sigma_i^2 \quad (\text{B11})$$

and

$$c_{fa} = 1 - \frac{1}{2} \sum_{i=1}^n \tau_i^2 \quad (\text{B12})$$

(B8) becomes

$$c_{fa} = 1 - \frac{1}{2} n \tau^2 \quad (\text{B13})$$

In the text, two cases are presented. In both, the correlation between two forecasts is roughly 98% at the stage that the correlation between a forecast and the analysis is 60% (namely at day 4 for the 8 April 1981 case, and at day 6 for the 7 September 1980 case). If one of the forecasts was useable as a verifying analysis, both (B8) and (B13) would give $\tau^2 = 0.04$ for $c_{fa} = 0.98$ and $n=1$. The number n of error fields required to reduce c_{fa} to 60% is then about 40 (B8) or 20 (B13) (all error fields have been assumed to have the same variance). Because of the many and bold assumptions involved, these numbers should not be considered anything more than an order of magnitude estimate.